

The new stereological tools: Disector, fractionator, nucleator and point sampled intercepts and their use in pathological research and diagnosis

Review article

H. J. G. GUNDERSEN, P. BAGGER¹, T. F. BENDTSEN, S. M. EVANS², L. KORBO³, N. MARCUSSEN,
A. MØLLER³, K. NIELSEN⁴, J. R. NYENGAARD, B. PAKKENBERG³, F. B. SØRENSEN, A. VESTERBY⁵
and M. J. WEST

Stereological Research Laboratory, University Institute of Pathology, 2nd University Clinic of Internal Medicine,
Institute of Experimental Clinical Research, University of Århus, ¹Laboratory of Reproductive Biology II,
University of Copenhagen, Rigshospitalet, ²Department of Psychiatry, University of Liverpool, England,
³Neurological Research Laboratory, Hvidovre Hospital, ⁴Institute of Pathology, University of Copenhagen,
Rigshospitalet, and ⁵University Institute of Pathology, Århus Amtssygehus, Denmark

Gundersen, H. J. G., Bagger, P., Bendtsen, T. F., Evans, S. M., Korbo, L., Marcussen, N., Møller, A., Nielsen, K., Nyengaard, J. R., Pakkenberg, B., Sørensen, F. B., Vesterby, A. & West, M. J. The new stereological tools: Disector, fractionator, nucleator and point sampled intercepts and their use in pathological research and diagnosis. APMIS 96: 857-881, 1988.

The new stereological methods for correct and efficient sampling and sizing of cells and other particles are reviewed. There is a hierarchy of methods starting from the simplest where even the microscopic magnification may be unknown to the most complex where typically both section thickness and the magnification must be known. *Optical* sections in suitably modified microscopes can be used to improve the ease and speed with which even the most demanding of these methods are performed. The methods are illustrated by practical examples of applications to a wide range of histological entities including synapses, neurons and cancer cells, glomerular corpuscles and ovarian follicles.

Key words: Disector; fractionator; nucleator; selector.

H. J. G. Gundersen, Stereological Research Laboratory, University Bartholin Bygning, DK-8000 Århus C, Denmark.

This is the second part of a review on New Stereological Tools by Gundersen & Coworkers.

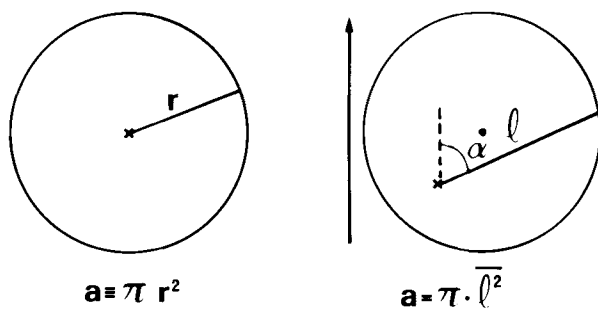
The first part appeared in APMIS, vol. 96, Number 5, May 1988, pp. 379-394.

COUNTING AND MEASURING IN THE REAL 3-DIMENSIONAL WORLD

The first part of this review (*Gundersen et al.* APMIS 96: 379-394, 1988, henceforth referred to as APMIS-1) dealt with a number of basic stereological principles for 2-dimensional quantitation and their use as tools for obtaining efficient and unbiased quantitative estimates of 3-dimensional structures. The methods required only a single,

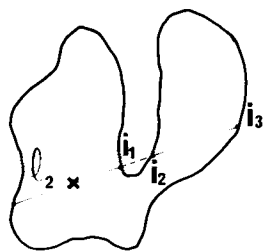
uniformly positioned thin section. With one exception, the methods in this second part of the review require *two* parallel sections which are often, but not always, of known thickness and specified orientation. The two sections need not be *physical* sections, i.e. physically separate, since optical sections suffice in almost all instances and are much more efficient, as described in detail below.

The methods described here represent a major



Independent of

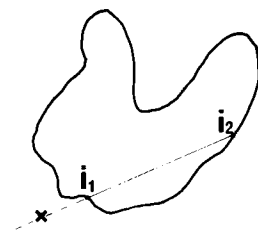
SHAPE



$$\ell_1^2 = \ell_{i_1}^2 - \ell_{i_2}^2 + \ell_{i_3}^2$$

$$a = \pi \cdot \bar{\ell}^2$$

POSITION



$$\ell_1^2 = -\ell_{i_1}^2 + \ell_{i_2}^2$$

$$a = \pi (\ell_1^2 + o) / 2$$

Fig. 1. The area of a circle may be estimated in two ways: $a \equiv \pi r^2$ and $a = \pi \bar{l}^2$, where the first is in fact just a special case of the latter. If the measured distance from the arbitrary point to the boundary varies with orientation one must measure in a random direction (uniform in the interval from 0° to 360°). The estimator is independent both of the shape of the profile and of the position of the point. For more than one intercept from the point one measures all squared distances to the boundaries and adds the ones which terminate over the profile and subtracts those which terminate on the outside of the profile. It is always an advantage to measure in both directions from the point. If the point is outside there are directions in which the measure is zero; they must also be taken into account in the mean, as shown.

breakthrough in Stereology because they are truly 3-dimensional and because they are the *only* stereological methods whereby particle number and sizes can be estimated in an unbiased manner. Before describing the principle on which this new and rapid development of Stereology is based, the

disector (Sterio 1984), it is necessary to describe a principle for measuring *n*-dimensional content and its spatial distribution. It was not described in APMIS-1 because it is as meaningless and useless in two dimensions as it is strong and versatile in three.

THE NUCLEATOR

We all learned in school that the area a of a circle is πr^2 , where the radius r is defined as the (constant) distance from the centre to the boundary. However, the same relation holds if we measure the distance l from *any* fixed point in the circle to the boundary, but only if the direction in which we measure is isotropic, see Fig. 1. Since the distance l now varies, the unbiased estimator of the area is $a = \pi \bar{l}^2$, i.e. if we measure in more than one isotropic direction the distances are squared before averaging. Note that $a \equiv \pi r^2$ is an identity because r is constant, whereas $a = \pi \bar{l}^2$ is an estimator with a certain coefficient of error, *CE*. Unbiasedness means, as always, that if we measure l in sufficiently many isotropic directions, the mean value of $\pi \bar{l}^2$ comes arbitrarily close to the true area (and the *CE* goes to zero). This old and well known relationship is true for *any* shape, however, and it does not require the fixed point to be in a specific position. The point may even be outside the profile, see examples in Gundersen 1988.

In 2-dimensional space this relationship is more of a curiosity (but how *was* it the planimeter worked?) than a working formula for estimating profile area, point counting is always likely to be more efficient, because we can see and sample the complete profile. In three dimensions it is quite another story. Ordinarily, we can only observe 2-dimensional sections and despite the notable efficiency of the Cavalieri-estimator of volume (APMIS-1) this estimator *does* require exhaustive sectioning of the object. The above estimation principle of the nucleator works, however, in any *n*-dimensional space: from an arbitrary, fixed point measure the distance l to the boundary in any isotropic direction and

$$\text{content} = c \cdot \bar{l}^n$$

where for $n = 1, 2, 3, \dots$ "content" is length, area, volume,... and $c = 2, \pi, \frac{4\pi}{3}, \dots$ (try it for $n = 1$!). For a 3-dimensional object, this means that the

TABLE 1. *The four stereological probes and the geometric characteristic they estimate in 3-dimensional objects*

Stereological Probe			Geometric characteristic of 3-dimensional object		
Name	Measure	Dimension	Name	Measure	Dimension
Point	number	0	Volume	volume	3
Line	length	1	Surface	area	2
Plane	area	2	Curve	length	1
Disector	volume	3	Cardinality	number	0

A list of the four basic stereological probes with indication of their measure (how to express the amount of the probe) and dimension. To the right the geometric characteristic of 3-dimensional objects to which the probe is “sensitive” (and therefore can estimate) is shown for each probe. Note the ambiguity of the word “volume”. A given probe of dimension k is a direct estimator of a d -dimensional characteristic only if $d = n - k$ where n is the dimension of the space embedding the object: 1-dimensional lines are therefore the principal probes for estimating $(3 - 1) = 2$ -dimensional surface area in 3-dimensional space. These are the principal or “primitive” relations where the estimation is performed by *counting* only, other relations exist as well. In fact, any k -dimensional probe can be used as an estimator of all geometric characteristics with dimension $d \geq n - k$, but not by just counting: the fractional length of test lines, L_L , is an estimator of both areal fraction A_A and volume fraction V_V , but one must *measure* the lengths of the intercepts. Note that whenever $d = n$ or $k = n$ one can perform the estimation *ignoring* the orientation distribution of both the probe and the object, in *all* other cases one has to know the orientation distribution of either object or probe. In practice this means that one must use *IUR* sections for estimating length or height with 2-dimensional planar counting frames and *IUR* lines on vertical or *IUR* sections for surfaces and for all direct size or distributional estimators based on the nucleator.

volume of the object can be estimated on just one section through the fixed point. The section must be either isotropic or fulfill the requirements for a “vertical” section to enable us to measure in isotropic directions in 3-dimensional space. Note that in practice the point must be unique and *recognizable* for it to remain in a fixed position independent of the direction of the section. These conditions can all be met in mononucleated cells, see Gundersen 1988, and, even more efficiently, in cells with just one nucleolus. Other structures may also be analyzed this way, cf. the follicle in Fig. 15 below. For many more details, proofs and a large number of closely related estimators, see Gundersen 1988. The nucleator principle: measurements carried out isotropically with respect to a fixed point, is very versatile. It is possible to estimate the *surface* of arbitrarily shaped, nucleated cells, Gundersen & Jensen 1987b. In addition, a whole range of other properties may be estimated as well, see Jensen *et al.* 1988, the example below illustrating *counting* with the nucleator, and Evans & Gundersen 1989a and Fig. 16 below illustrates how it can be used to estimate the *spatial distributions* of *all* these quantities. However, before going into more details it is first necessary to describe

how to *sample* particles uniformly, of necessity the first step in analyzing them.

THE DISECTOR: HOW TO SAMPLE OBJECTS UNIFORMLY

Humans have five senses like most living creatures: Smell, sight, touch, taste, and hearing. We do not generally get confused because a given object (a dead fish, maybe) is both visible, stinking and feels slimy at the same time. These are different qualities (modalities) of the same object. As opposed to most lower species, stereologists have at least four extra senses or probes which are sensitive towards and very specific for four geometric modalities of 3-dimensional objects: volume, surface, length, and number, see Table 1. The real problem used to be that no probe can estimate a characteristic of dimension *less* than the $(n - k)$ dimensions of its principal target. Therefore none of the first three probes listed in Table 1 (i.e. those reviewed in APMIS-1) can estimate 0-dimensional number, only the 3-dimensional disector “feels” number without regard to volume, shape or height of the isolated objects.

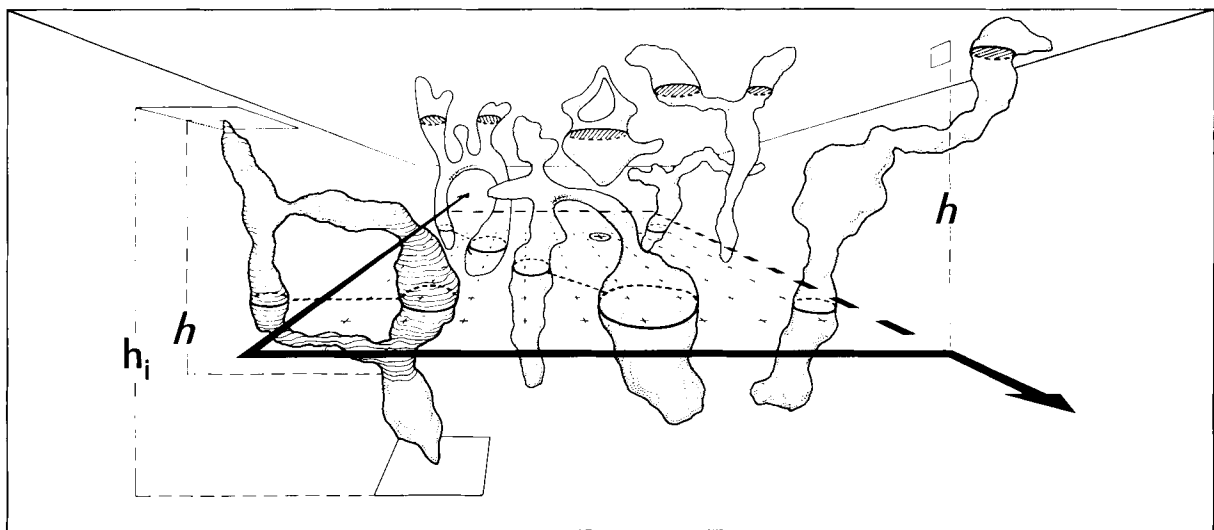


Fig. 2. The disector. Two parallel section planes a known distance h apart with an unbiased counting frame of area $a(\text{frame})$ on the sampling or reference plane. Complete transects (one or more profiles in the same particle) are sampled if they are partly or totally inside the frame provided they do *not in any way* intersect the fully drawn exclusion edges or their extension. There are $Q = 4$ such transects sampled in the Figure. Of these four, two are intersected by the upper look-up plane and are *not* counted. The number of particles in the probe is the remaining $Q^- = 2$.

Like the unbiased 2-dimensional sampling and counting frame show in Fig. 2 and described in APMIS-1, the disector is a probe which samples isolated objects or particles with a uniform probability in 3-dimensional space, irrespective of their size and shape. The disector is shown in Fig. 2. The section pair must have uniform position in the reference space, the space which contains the particles, and generally the sampling frame must have a (systematic) random position in the reference section. The precise rule for sampling particles is given in the legend to Fig. 2, see also the original description (Sterio 1984) and the review of the disector and many other estimators based on this principle in Gundersen 1986. For an uncovering of the almost 100-year-long history of the disector-principle, see Bendtsen & Nyengaard 1988.

“Sampling particles with uniform probability” means that *a priori* all particles have the same chance of being sampled. The set of particles actually sampled therefore constitutes a “fair” or “representative” or uniform sample of all particles. In practical terms, this means that the mean characteristic of the sample is an unbiased estimate of the same mean characteristic of *all* particles in the reference space. This simple and immutable fact is the basis for many of the applica-

tions of the disector. The height h of the disector (usually the thickness of one of the two adjacent sections) need *not* be known – sampling is uniform anyhow. A disector-sample is the *only* stereological sample of particles which has this extremely important feature of uniformity. Specifically, a sample of cells taken because they were hit by a single section is *not* a uniform sample. Such a sample is height-weighted: a cell which is twice as high as another has twice the chance of being in the sample. This is worth emphasizing: *the cells (particles) seen in a single section is a biased, non-representative sample of all cells*.

The simplest use of a sample is to *count* the Q^- elements in it. Knowing the magnification and the height h , the volume $v(\text{dis})$ of the disector-probe is known: $v(\text{dis}) = a(\text{frame}) \cdot h$ and a straightforward estimator of the total number of particles in a specimen of volume $V(\text{ref})$ is:

$$N(\text{particles}) = \frac{\sum Q^-}{\sum v(\text{dis})} \cdot V(\text{ref})$$

where the summation is over a number of systematically sampled dissectors in the reference space. In biology, the tissue surrounding the particles to be counted or sampled is almost always transparent and the section thickness may therefore be larger than the minimal diameter of the particles to be

counted (*Sterio* 1984). In order to identify and distinguish different particles correctly one should rarely use a section thickness exceeding 1/4 to 1/3 of the height of the particles, which in practice is the more important constraint on section thickness. If the particles are sparsely distributed one may use slightly thicker sections, whereas for densely packed particles one may have to use very thin sections – or rather *optical* disectors if this is at all possible. The two situations are illustrated in Figs. 4 and 15 which show neurons and follicle granulosa cells, respectively. (Some special problems arise when the *absence* of something is counted, e.g. holes in perforated synapses, see *Calverley & Jones* 1987) In many cases one may take advantage of the freedom to use a particularly “good” direction for identifying the particles to be counted, see for instance *Mulvany et al.* 1985, who counted smooth muscle cell nuclei in arterioles on sections parallel to the vessel axis and thereby perpendicular to the long, curved cell nuclei. Sectioned this way it was much easier to identify the nuclei.

Undoubtedly the most common question asked by investigators starting stereological projects is: “How many must I count?”, i.e. points, intersections, profiles or particles. The answer is simple: “never count more than 100 to 200 (and that only in extreme cases) in one biological unit (often an organ)!”. For a general consideration of this, see the discussion and review in *Gundersen* 1986, *Gundersen & Jensen* 1987a, *Michel & Cruz-Orive* 1988, and the detailed example and calculation of the pertinent CEs in *Pakkenberg & Gundersen* 1988. To our knowledge, a counter-example of this rule based on a statistical analysis of sampling designs has never been published.

THE OPTICAL DISECTOR

The idea of the optical disector (Fig. 2.3 in *Gundersen* 1986) is to start by making only *one*, relatively thick section, ~ 25 µm, say, and then make the two or more parallel section planes for the disector as thin *optical* sections inside the thick one by moving the plane of focus up or down. Optical sectioning greatly facilitates the application of most of the new stereological techniques described in this review. Optical sectioning will be at its best when used on a confocal microscope, see e.g. *Petran et al.* 1968 and *Howard et al.* 1985, a

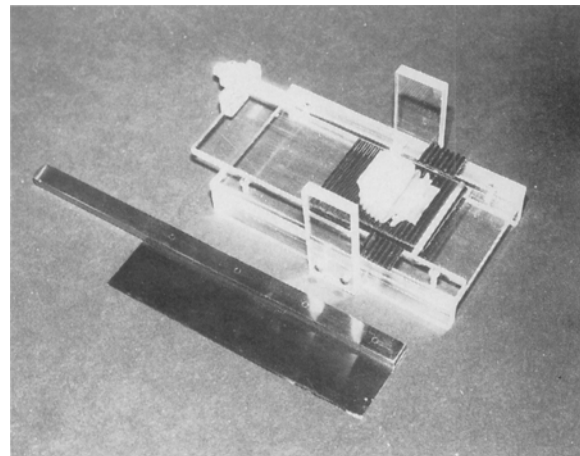


Fig. 3. The modified Olympus BH-2 microscope has an electronic microcator (Heidenhain, VRZ 401) attached to the side (M), and a projection arm. The light source is a 100 Watt halogen light bulb which is housed in a modified lamp housing to maximize its illuminating power. A set of motors (not shown here) is usually attached to the specimen stage for stepwise, predetermined movements in the x- and y-direction to aid in the systematic sampling of fields of view. There is a special rotating stage fitted (see Fig. 9 in APMIS-1) so that specimens can be rotated through 360° independently of the x,y-movement of the stage (When in use, the projection is onto test-systems on the table surface).

wonderful invention which still does not work in transmission, only in reflectance or fluorescence illumination mode. Almost all the methods illustrated below have therefore been carried out in thick plastic sections on a conventional light microscope which in various ways has been modified for stereological use, see Fig. 3.

The two main modifications are an electronic microcator which has been fitted to the microscope to measure the movements of the stage in the z-axis and that the microscope is fitted with a projection arm. High numerical aperture oil immersion lenses, with a matched numerical aperture condenser give the smallest possible focal depth. Only oil immersion lenses should be used for optical sectioning because the movement of the specimen stage, which the microcator measures, then equals the movement of the plane of focus (provided the refractive indices of the embedding medium and of the immersion oil are equal). Using glycolmethacrylate and, for example, a standard Giemsa staining, the thickness of the physical section can be varied from 0.5 µm to more than 100 µm without problems. Although disec-

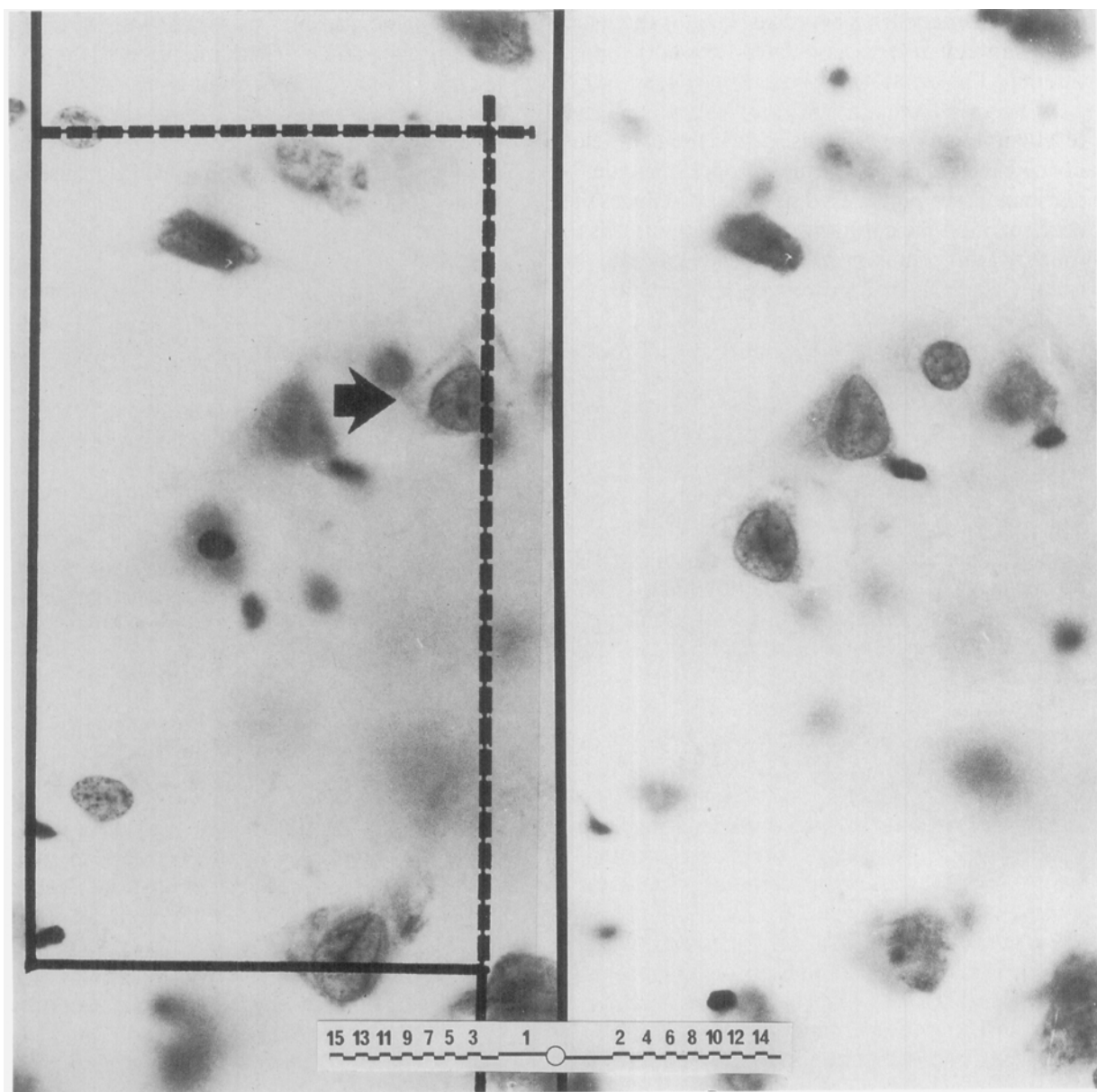


Fig. 4. Two optical sections 2 μm apart in the middle of a Giemsa stained glycolmethacrylate section of $\sim 25 \mu\text{m}$ thickness. In an appropriately (systematically) sampled microscopic field, one focuses down $\sim 5 \mu\text{m}$ to avoid distortions and unevenness of the section surface. All neuron nuclei seen in focus in this look-up plane to the right are disregarded. Then one focuses through a distance of e.g. 10 μm in 2 μm steps counting any neuron nucleus which comes into focus, including those in the last optical section. A neuron is counted or sampled when its clearly focussed nucleolus is counted in the disector sampling frame as shown to the left. A non-negligible fraction of small neurons in human cortex do not have a well-defined nucleolus, potentially quite a problem when in the old days neuron nucleoli were counted in *one* section only (?). By contrast, in the optical disector one focuses through the nucleus and observes the lack of a nucleolus and instead simply counts these neurons when their sharpest nuclear profile falls within the disector counting frame. The physical section should be sufficiently thick to allow a guard volume of a few μm thickness at the bottom of the disector for resolving ambiguities in identification and to avoid the problems of lost caps. The frame size is 67 μm by 137 μm . The ruler used for classifying intercepts to either side of the nucleolus or nucleus centre (for nucleator-estimates of neuron volumes) is shown below at ~ 3 times normal size. It is constructed like the one shown in Fig. 6.

tors can be made from physical sections there are important advantages associated with optical sectioning. The most time consuming step when using physically separate sections as disectors, that of aligning the two sections so that the two fields of view in two identical microscopes coincide, is eliminated, see Fig. 4. This simple fact reduces the time spent on the counting or sampling of cells to roughly a fifth, making it possible to estimate for example the total number of neurons in a human brain cortex with a *CE* of ~ 5 per cent in less than half a day; and the estimate is then even made for separate cortical areas (*Brændgaard et al.* 1989). The extra information obtained from working in three dimensions also makes the identification of individual structures much easier. In fact, very densely packed cells like granule cells in cerebellar cortex and granulosa cells in follicles, see Fig. 15, are almost impossible to count in *physical* disectors. Moreover, since the microcator is fitted to the side of the microscope, the height of a disector is measured directly, (the electronic microcator has an accuracy of more than 0.5 μm) thereby avoiding the problem of elaborate calibration of the microtome or of measuring the thickness of the physical section.

Cells with more than one nucleus or more than one nucleolus used to present a rather awkward problem when applying the disector or the nucleator principle, since both techniques are only effortless to apply when the particle contains something unique inside. So it is another advantage of optical disectors that given sufficient section thickness, one can sample nuclei or nucleoli in the middle 5 to 10 μm of the section and then use the rest of the thickness to ensure that sampling was unique and thereby uniform by looking through the sampled cells and determining the number of nuclei or nucleoli in them, see *Vesterby* 1989 for an example of polynucleated cells.

POINT-SAMPLING OF NUCLEAR INTERCEPTS IN CANCER GRADING

The principal sensitivity of a probe to a certain geometric characteristic, listed in Table 1, is a feature which is used directly in the estimation of these characteristics. The sensitivity of a probe is also used in sampling schemes, most directly in the sampling of particles. As mentioned above, one

section plane samples particles with a chance proportional to their linear dimension ("length" or height), a sampling scheme only of interest here because it produces a *non-uniform* sample of a type at which almost all microscopists look every day. Sampling particles with points has been used in geology and materials sciences for many years. This type of sampling was revived for biological use a few years ago (*Gundersen & Jensen* 1983 and 1985). Random points thrown on a randomly positioned section hit a particle with a probability which is directly proportional to the volume of the particle. Sampling therefore only cells hit by random points, one studies a *volume-weighted* sample of cells or a sample of cells from the volume-weighted distribution.

There are two good reasons for using this special sampling technique in certain areas of research and diagnosis. In biology there are many instances in which one might expect the largest particles to carry the most information about a certain change. Studying a sample of cells which contains a larger fraction of big nuclei than a uniform sample might therefore lead to a greater sensitivity in detecting early or relatively small changes (*Gundersen* 1986). Another reason for using point sampling as opposed to uniform sampling with the disector, is that it requires only *one* section. An attractive feature of this scheme is that the point-sampled particles in the section can then be studied by the nucleator sizing-principle on the *same* section. When, in the description of the nucleator, it was stressed that the point must be unique and recognizable, the reason was mainly to ensure correct *uniform* sampling with the disector. In an already sampled cell the nucleator sizing principle works for any point inside the cell, including a random sampling point. Since the point is random inside the particle, it is not efficient to make two measurements in two opposite directions from the point, it is better to measure the length of the *complete intercept* through the point in a 3-dimensionally isotropic direction (on *IUR* or "vertical" sections). The coefficient to be used for calculating the volume-weighted mean particle volume \bar{v}_V is then $\frac{\pi}{3}$ instead of $\frac{4\pi}{3}$. This special case of the general nucleator principle was described before the nucleator and has its own name, *point-sampled linear intercepts*, which also describes reasonably precisely what it involves.

One of the most uniform features of many malignant cell populations is the change in their

nuclear morphology: the appearance of cells with nuclei which are quite large. Since the absolute size is difficult to judge with any precision, the variability of nuclear size between cells may often be the most telling feature. Tumours with very large cell nuclei or showing a pronounced variability of nuclear size will generally be deemed more malignant. It is well recognized among pathologists that the subjective assessment of these changes on a qualitative scale is not very reproducible. Various quantitative methods have therefore been used with varying success (e.g. Helander *et al.* 1984, and Ooms *et al.* 1985), but most of these have used only 2-dimensional quantities as a basis for making decisions. Such techniques are unlikely to be optimal for 3-dimensional changes in 3-dimensional structures.

In routine histopathology many sections of tumours fulfill the criteria for uniform random point sampling and isotropically oriented test lines. Tissue chips from tumours, e.g. from bladder tumours and from prostatic tumours may be assumed to be approximately randomly oriented during the embedding procedure. This means that routine sections of such tumour specimens for all intents and purposes are IUR sections. One may then use a sampling probe of systematic points on lines in any, fixed direction (parallel to the edge of the table, for example). Using such a test system ~ 75 intercepts are classified on 5 to 10 fields of vision using a projection microscope such as that shown in Fig. 3. This classification takes less than 10 minutes per tumour using the ruler shown in Fig. 6. Knowing the magnification and the physical length of the ruler one calculates the mean, cubed intercept length, as described in detail in Brændgaard & Gundersen 1986, and obtains the estimate $\bar{v}_V = \frac{\pi}{3} \cdot l_0^3$. The CE depends on tumour type and grade but it is mostly in the range 0.1 to 0.3, a satisfactory level for routine use in single patients and for scientific purposes. It should be noted that this estimate of the mean nuclear volume is both objective and very reproducible (Nielsen *et al.* 1988a).

A good correlation between the mean nuclear volume in bladder tumours and the prognosis is present. With arbitrary cut-off points of < 300 μm^3 , 300 to 500 μm^3 , and > 500 μm^3 80 patients were divided into three subgroups with 35, 26, and 19 patients, respectively. Five years after the diagnosis, 1, 7, and 18 in the respective subgroups had died from their cancer (Nielsen *et al.* 1986). In a

\bar{v}_V (nuclei) in first, benign bladder tumour

	≤ Median	>Median	Σ
No recurrence (10 years)	9	1	10
Recurrence, No invasion	7	4	11
Invasion	2	12	14
Σ	18	17	35

Fig. 5. The recurrence pattern in a ten-year follow-up period in 35 patients with urinary bladder papilloma as a function of the volume-weighted mean nuclear volume in the first biopsy. The median \bar{v}_V of the group is 165 μm^3 . The areas of the black rectangles are proportional to the frequency in each row. Modified from Nielsen *et al.* 1988b.

time where resources for health care seem to become more scarce, it may also be of value for the distribution of these resources that another study showed a very strong relation between the mean nuclear volume in a patient's first bladder papilloma and the probability that over the next 10 years the patient 1) would not develop a new tumour or 2) would develop one or more tumours which would not become invasive or 3) would develop invasive bladder cancer, see Fig. 5 and Nielsen *et al.* 1988b. Biologically, it is remarkable that although all patients had their initial tumour removed, the nuclear \bar{v}_V of the first tumour nevertheless was closely related to the malignant potential of the next tumour(s), making it possible to assign a different frequency of control visits to the clinic on the basis of the first biopsy.

In the above example, the isotropic orientation of the section plane was easily made (see also the "Cucumber" Orientator by Mattfeldt in APMIS-1) and was easy to use. There are, however, a number of tissues where too much information about the precise location of the samples is lost on IUR sections, as in tubular systems or surface epithelia like the example of a benign cutaneous naevus described here. The advantage of the vertical section design is that the tumour is sliced into vertical sections (systematically around the vertical axis for optimal sampling, see APMIS-1),

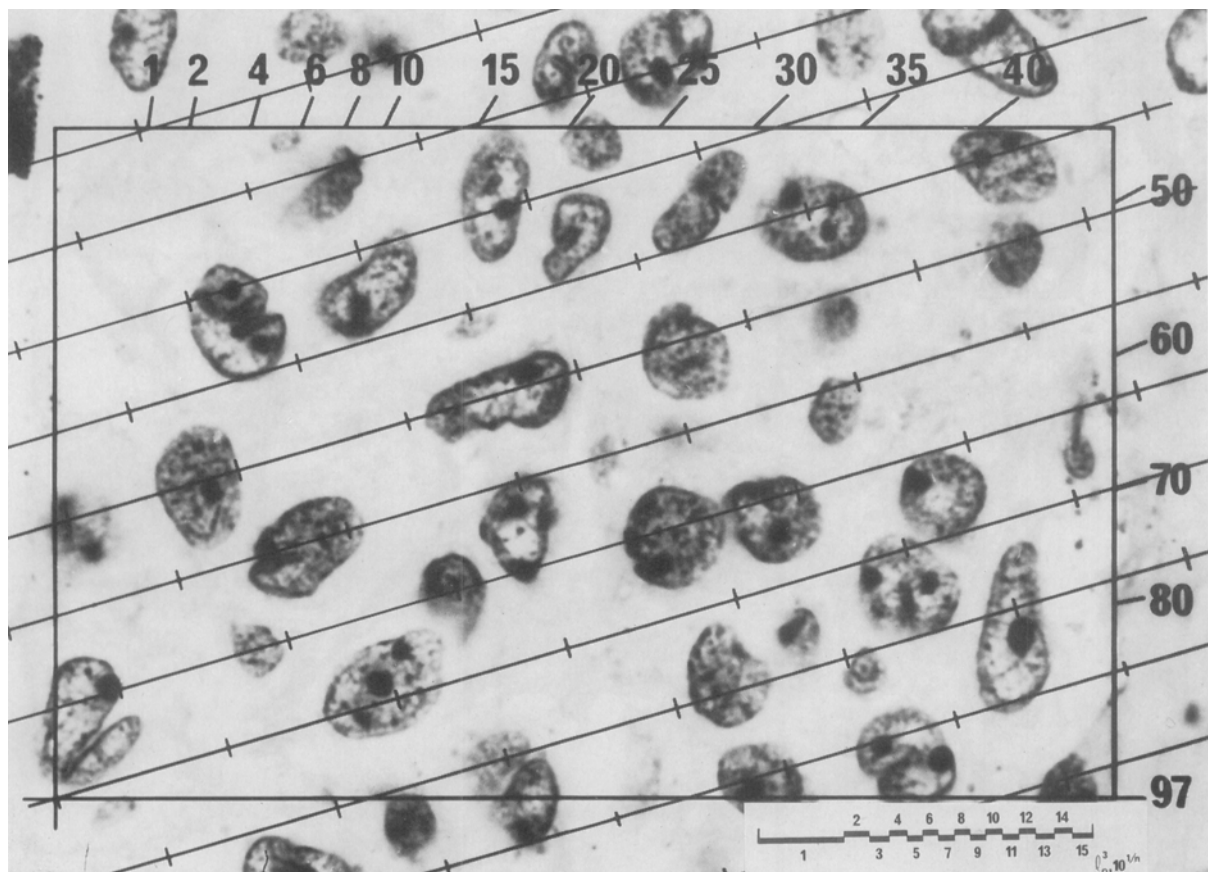


Fig. 6. A vertical section of a benign cutaneous naevus projected onto the test system for vertical sections. The vertical axis has been aligned with the left hand edge of the orientation frame at a lower magnification. For each point inside the frame which hits a nucleus, the nuclear intercept through the point is measured in the direction dictated by the test-line. All points which fall inside the frame are considered (also if they hit a nucleus which is on the edge of the frame) whereas points falling outside the frame are ignored. The direction-number for the first field is a random number between 1 and 97, in the Figure 70 was obtained from a random number table, e.g. page 131 in Documenta Geigy, Scientific Tables, 7th ed., Diem & Lentner 1970. For each of the following fields of vision a new direction-number is obtained by adding 37 to the previous number or, if the sum is > 97 , subtracting 60. The next numbers after 70 are therefore 10, 47, 84, 24, etc. (Giemsa stain, original magnification: 1500X). In the Figure a classified ruler for measurements of intercepts is also seen. The ruler is made with a scale of volume or length raised to the third power to obtain cubed intercept lengths directly. The widths of the first and the 15th class have a ratio of 10:1, i.e. on the volume scale the 15th class is ten times wider than the first, almost the opposite of the physical ruler seen here on an of necessity linear scale. Due to this construction, the ruler classes are differentiated and handy to use, for instance in sections of nuclear populations showing size-pleomorphy, see also Fig. 10 where an even more differentiated ruler was used.

perpendicular to the horizontal plane of reference which is the macroscopical epidermal surface. Vertical histological sections are projected onto a table at a final magnification of $\sim 2000X$ using the projection microscope shown in Fig. 3. Nuclei are point-sampled and the point-sampled intercept lengths are measured according to the principle used for isotropic sections. The crucial step is the construction and application of a test-line system

which satisfies the requirement for three-dimensional isotropic test-line directions. In brief, test-lines with a greater angle to the vertical axis must be selected with greater frequency than those close to the axis. For the practical implementation of such a system a "direction-finder" or orientation frame can be constructed, see Fig. 16 in APMIS-1, where the left-hand edge is always aligned with the chosen vertical axis. A transparent test-system

with points and lines is then superimposed on the orientation frame with a systematic random choice of direction-number, see Fig. 6. Any ruler may be used for the measurements of intercepts, but a handy ruler construction whereby one actually obtains cubed intercept lengths is also shown in Fig. 6. Detailed description of the ruler design and calculated examples of \bar{v}_V are found in Brændgaard & Gundersen (1986) and Sørensen (1989c). Estimates of the volume-weighted mean nuclear volume from vertical sections of cutaneous melanocytic tumours (Howard 1986, Brügger & Cruz-Orive 1987, and Sørensen 1989a & 1989b) turn out to be closely related to the tumour type. More importantly, it is also highly correlated to the patients' five-year survival, even in a homogeneous group of patients with malignant melanomas all in stage 1, see Sørensen 1989a & 1989b.

Estimates of nuclear \bar{v}_V may be of especially great value in the search for objective malignancy grading parameters in various cancers. One reason why the estimator is a very sensitive parameter is that it *combines information on both mean nuclear size and variability of size*, since $\bar{v}_V = \bar{v}_N \cdot (1 + CV^2_N(v))$ where \bar{v}_N is the mean volume in the ordinary number distribution and $CV_N(v)$ is the coefficient of variation of particle volumes in the same distribution. In fact, by estimating nuclear volume in both the number distribution and the volume distribution *nuclear pleomorphy* may be defined quantitatively, another promising prospect within the field of future objective malignancy grading (Sørensen 1989c).

THE FRACTIONATOR

In the rest of the methods in this review particles will be considered as individuals of equal importance, i.e. mean volumes are estimated in the number distribution and total number is also a parameter of direct importance. All the methods therefore rely on the disector as the primary sampling device. In most of the examples the disector is used in a very direct way without knowing for instance the section thickness. The simplest of these sampling schemes is the Fractionator, which in fact is the simplest of all sampling schemes known in Stereology and for that very reason also the most powerful. Except by deliberately cheating, it is not known how to make a

biased fractionator!

When estimating the number of particles in a pathological specimen, it is usually impractical to count them all. Instead the particle number is estimated in a known fraction of the reference space. The fractionator principle involves sampling particles *uniformly at random* with a *known and predetermined* probability, and then deriving the total number N in the reference space from the number in the sample and the sampling probability (Gundersen 1986, but the principle has been known outside the field of Stereology for a long time, see Jolly 1979). An organ containing particles is cut into pieces of unknown number, size and shape. A known and predetermined fraction of the pieces is sampled randomly (e.g. a fifteenth of all pieces is taken systematically with a random start). Because any particle is contained in one of the segments, every particle has the same probability of being sampled, i.e. sampling is *uniform*. N can then be derived as the product of the particle number in the sample (N') and the inverse sampling probability: $N = N' \cdot 15$. This is an unbiased estimate of N . The sampling can be performed in two or more steps. In a large organ one may conveniently start by cutting it into a set of thick slabs, sample a fraction of them, cut these into bars, sample again from the bars, and cut the bars into small blocks of which a sample is then taken. This only takes a couple of minutes. The blocks are then embedded and sectioned *exhaustively*. However, one need sample only a small fraction of all sections (and a look-up section for each sampled section). In the last step one may then sample every tenth field of vision in every tenth row in a systematic design and in these fields count nuclei or glomeruli seen in one section and not in the other. The total number of counted particles times all the inverse sampling fractions is an unbiased estimate of N . If in the above steps a tenth to a hundredth was taken at each step one only counts from $\sim 1/100,000$ to $\sim 1/1,000,000,000$ of the particles – that is not a lot of work even in a whale kidney! The most remarkable feature of the fractionator is, that any need for dimensional information, like section thickness or magnification, is eliminated and the estimate is therefore independent of tissue deformation like shrinkage or swelling – even differential shrinkage does not influence the unbiased nature of the estimator. Note that in the disector one *estimates* the sampled fraction = $\frac{\Sigma v(dis)}{V(ref)}$ and shrinkage of the specimen

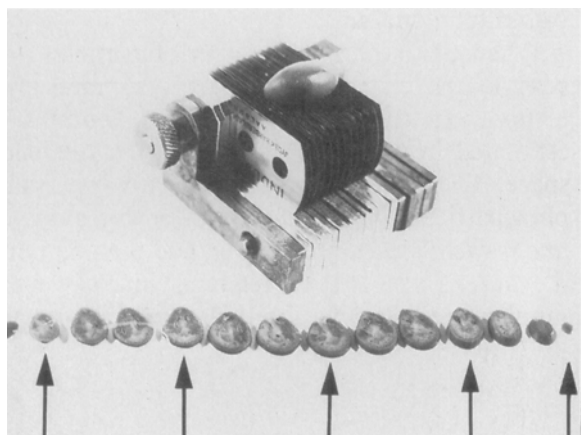


Fig. 7. A rat kidney is cut into a series of slabs of roughly the same thickness using the "razor blade fractionator". The slab to be sampled first is found by means of random numbers. Here the aimed fraction is *a third* of the kidney. A random number between 1 and 3 is chosen (here no. 2). This slab and every third slab is sampled, here 2, 5, 8, 11, and 14. Statistically, this set of slabs contains on average exactly a third of everything in the kidney.

during dehydration and embedding *after* estimation of $V(\text{ref})$ may well be a problem for this estimate to be unbiased. See the discussion of this problem and a very simple elimination of it for small organs in *Pakkenberg & Gundersen 1988*.

Whenever differential shrinkage might be a problem when comparing normal and diseased tissue or when paraffin embedding is used, the fractionator may well be the simplest (and an excellent) solution to *all* such problems.

Repeated estimates of the number of particles in the reference space will provide results varying around the true value. The efficiency of the fractionator (a low CE) depends on 1) homogeneity of the particle density in the reference space, 2) any random variation in the size of the pieces (the effect of their systematic variation is essentially limited by the systematic sampling), and 3) the number of pieces which are actually sampled (*Gundersen 1986*). The efficiency is improved by systematic sampling from a row of segments, see Fig. 7 and *Gundersen & Jensen 1987a*. The actual CE of a certain sampling scheme may be estimated rather easily, see Eq. 2.11 in *Gundersen 1986* and the examples in *Nyengaard & Bendtsen 1989a* and *1989b*.

In these studies the CE was estimated in groups of 8 and 25 systematically sampled, double esti-

mates in animal and human kidneys. Both series showed a CE of ~ 11 per cent, based on a mean glomerular count of 135 and 107 per kidney, respectively. The CE is therefore almost as low as one could expect it to be, under independence and uniformity the expected CE on a count of 121 is $\sim \frac{1}{\sqrt{121}} = 9.1$ per cent. There are 600,000 and 23,000 glomeruli per kidney in man and rat, respectively (*Nyengaard & Bendtsen 1989a* and *1989b*).

THE SELECTOR – ESTIMATING THE VOLUME OF PARTICLES AND ITS VARIATION IN A DISECTOR OF UNKNOWN THICKNESS

The selector is the first of a series of techniques by which particle size and number may be estimated if just the magnification is known. It is based on a combination of the disector and the point-sampled intercepts and was first described by *Cruz-Orive* in 1987 in a paper which provided much impetus for the nucleator. Its principle is deceptively simple. In a stack of sections higher than the highest particle but otherwise of unknown and possibly varying section thickness, the first two sections are used as a disector for sampling n particles. These particles are followed through all the next sections, projected onto a systematic set of points, and complete intercepts are measured through every point hitting a sampled particle, see also the descriptions in *Cruz-Orive 1987* and *Gundersen 1986*. All n sampled particles must be hit with a test-point at least once; if more than one intercept is measured in a particle one calculates the simple mean of the cubed lengths for that particle, $\overline{l_{0,i}^3}$. Since $v_i = (\pi/3) \cdot \overline{l_{0,i}^3}$ is an unbiased estimate of the volume of the i 'th particle, it follows that

$$\overline{v_N} = \frac{\pi}{3} \cdot \frac{1}{n} \cdot \sum_{i=1}^n \overline{l_{0,i}^3}$$

is an unbiased estimate of the mean volume of the particles from the number distribution of particle volume: The particles were sampled uniformly in a disector. An example with rat Purkinje cells is shown in Table 2.

Once the mean volume in the number distribution is known, a range of other estimates are possible. With an estimate of the reference volume $V(\text{ref})$, from either the Cavalieri-estimator or by just weighing the specimen, and of the volume

TABLE 2. Point-sampled intercepts in disector-sampled Purkinje cells followed on consecutive sections

Cell no.	Section no.	2	3	4	5	6	k	$\sum_{j=1}^k l_{0,i}^3$	$\bar{l}_{0,i}^3$
1		30.7					1	30.7	30.7
2			68.0	21.8;14.3			3	104.1	34.7
3		30.7	41.1		30.7	14.3	4	116.8	29.2
4		30.7	41.1;30.7	2.5;14.3			5	119.3	23.9
5		68.0	7.9	2.5			3	78.4	26.1
6		41.1					1	41.1	41.1
7		41.1	41.1	53.5	14.3		4	150.0	37.5
8		30.7	30.7		2.5		3	63.9	21.3
9		7.9	41.1	53.5	53.5	105.3	5	261.3	52.3
10		30.7	30.7	21.8		53.5	4	136.7	34.2
11		2.5	21.8	53.3		41.1	4	118.9	29.7
$\Sigma n = 11$							37	1221.2	360.7

$$\bar{l}_0^3 = \frac{\sum_{i=1}^n \sum_{j=1}^k l_{0,i}^3}{\sum_{i=1}^n k} = \frac{1221.2}{37} = 33.0 \text{ } u^3$$

$$\overline{\bar{l}_{0,i}^3} = \frac{1}{n} \sum_{i=1}^n \bar{l}_{0,i}^3 = \frac{1}{11} \cdot 360.7 = 32.8 \text{ } u^3$$

$$CV_N(v) = \sqrt{\frac{\bar{v}_V}{\bar{v}_N} - 1} = \sqrt{\frac{33.0}{32.8} - 1} \sim 0.09$$

Eleven Purkinje cells sampled from an IUR stack of sections in rat cerebellar cortex. All cells seen in a random field of view in the second section but not in the first are sampled. On the second section and all following sections wherein the sampled cells (perikarya) are seen a set of systematic points is thrown at random. Through all points hitting the sampled cells the cubed length of the intercept $l_{0,i}^3$ is classified using the ruler shown in Fig. 6; these measurements are shown for each cell. A cell may be present in a section without being hit by a point and may also be hit by more than one point in a section. Each time a point hits a measurement is performed. The mean cubed intercept length $\bar{l}_{0,i}^3$ is calculated for each cell in the last column, the average of these 11 means times π is an unbiased estimator of the mean Purkinje perikaryan volume: $\bar{v}_N = \frac{\pi}{3} \cdot \bar{l}_{0,i}^3$. Taking the magnification and the ruler construction into account the arbitrary ruler unit u^3 shown here equals $71.5 \mu\text{m}^3$, i.e. $\bar{v}_N = 32.8 \cdot 71.5 \mu\text{m}^3 \sim 2350 \mu\text{m}^3$. The formula at the end of the table shows how to estimate the relative variation $CV_N(v)$ in the ordinary (number) distribution of perikaryan volume. Note that for this estimate one need not even know the magnification.

fraction $V_V(\text{par}/\text{ref})$, from simple point-counting, one may estimate (indirectly) the total particle number by $N(\text{par}) = V(\text{ref}) \cdot V_V(\text{par}/\text{ref}) / \bar{v}_N(\text{par})$ still without knowing the section thickness. It is, however, a much more useful property of the selector that one may obtain a rather straightforward estimate of the *relative variation in the number distribution of cell volumes*, because both \bar{v}_N and \bar{v}_V are known, see Table 2. \bar{v}_V is estimated by the average of *all* measured intercepts, no matter which particles they come from, see the example in Table 2. It appears that Purkinje cells in adult rats

are relatively uniform in size with a $CV_N(v) \sim 0.1$, but a sample of only 11 cells may be a trifle too small to be certain!

The selector is a relatively efficient estimator of the variation in cell volume because the ratio between the two mean volumes \bar{v}_V/\bar{v}_N is estimated in the same cells. As in all other paired sampling designs, this eliminates a lot of sampling variation in the estimate. One should consider, however, that in most situations the disector is a more efficient estimator of particle numbers and the nucleator a more efficient estimator of size than the selector

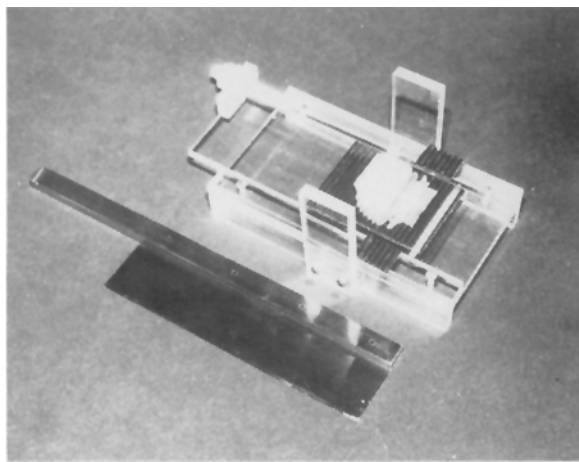


Fig. 8. Instrument for cutting small items macroscopically. The tissue is fixed to the horizontal, ruffled plate with 7 per cent agar. For optimal fixation the tissue must be put into the warm agar for a few minutes. The stability during cutting is best if the agar block is kept at $\sim 5^\circ\text{C}$ for some hours and cut while cold. The plate can be advanced between cuts at intervals of 1/6 mm using the threaded bolt at the end.

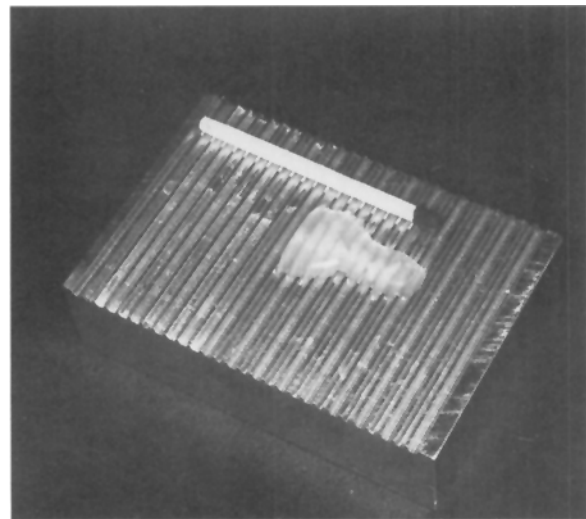


Fig. 9. Solid block of aluminium with semicircular grooves of a depth of ~ 2 mm. When the block is kept at $\sim 40^\circ\text{C}$ for some time before the tissue is fixed to it with 5 per cent agar it is relatively easy to put the tissue rods parallel and with a random rotation for vertical sectioning.

for which a whole stack of serial sections has to be studied. The fact that one need not know the section thickness is of minor practical importance when using the optical disector. If cell volume variability is a parameter of major importance, it is probably more efficient to use Cavalieri's estimator on each cell in a stack of serial, *optical* sections (see the example with the nucleator in human cortical neurons below, and Fig. 4.1 in Gundersen 1986 for a very simple solution to the overprojection which occurs when transmission (projection) is used for the Cavalieri-estimator).

THE NUCLEATOR ON VERTICAL SECTIONS

When the nucleator is used on vertical sections it is possible to optimize the preservation of information about where the particles are sampled. This might, for example, be of importance when estimating the neuron perikaryon volume, since there is a pronounced variation in neuron size in the different layers of the cerebral cortex, and various disorders may well affect neurons in a particular layer. The example here is from the cerebral cortex of a rat, it is also used to illustrate some of the short-cuts possible in the method which reduce the workload considerably. For this reason a disector

with two physical sections was used.

A rat brain hemisphere is embedded in agar and sliced into 1.5 mm coronal slices (Fig. 8). The volume of the cortex is estimated according to the Cavalieri-principle, see APMIS-1, using a test-system with a point-spacing of 1.0 mm at 20 X magnification using a dissection microscope (Olympus VE3). Each slice is cut in 1.5 mm wide, parallel rods, which are roughly perpendicular to the pial surface, approximately 50 rods in all. With a random start every sixth piece is sampled and embedded in agar in the indentations on the device shown in Fig. 9, with all pial ends in the same direction. Each rod is randomly rotated around its longitudinal axis, see also Fig. 8 in APMIS-1. The agar block is then dehydrated and embedded in glycolmetachrylate and two pairs of 3.5 μm sections from the middle of the block are Giemsa-stained. The section pairs are viewed in two microscopes projecting the images onto the table at $\sim 1600 X$. Neuronal nuclei which have their nucleolus in an unbiased frame in one section but are not present in the other section are sampled. Due to the vertical section design, directions in which to measure must be sine-weighted using the frame shown in Fig. 6. The vertical axis is clearly identifiable as the axis of the rods. The neuron nuclear and perikaryon volumes are estimated as

shown in Figs. 4 and 6. The mean volume of neuronal nuclei is $\sim 500 \mu\text{m}^3$ and that of neuronal perikarya is $\sim 1040 \mu\text{m}^3$. A surprisingly close relationship is present between the volume of individual neuron perikarya and the volume of their nuclei, $r = 0.95$ (*Møller & Gundersen* 1989).

All the neuronal nucleoli have the same chance of being sampled with the disector, regardless of variations in size (height). There is, in fact, some variation in nucleolar size, the largest nucleoli are seen in the largest neurons which also have the largest nuclei. On an absolute scale the diameter variation is $\sim 1 \mu\text{m}$ which is not very large compared to the section thickness of $\sim 3 \mu\text{m}$. The effect of selecting in *one* section *all* neurons which showed their nucleolus was therefore studied. As expected, the latter method leads to an overestimate of perykaryon volume: the largest neurons have a greater chance of being sampled. However, the bias was only ~ 3 per cent. This means that for a number of studies one might just sample neurons in *one, independent section* and estimate their volume in the same section with a very small bias, a bias which can be quantitated in a moderate number of animals. This is a great advantage when using stains which do not penetrate the thick plastic sections necessary for the optical disector. For a detailed description of this and a range of other time saving short-cuts, see *Møller & Gundersen* 1989 and *Gundersen* 1988.

ESTIMATING THE SIZE DISTRIBUTION OF CELLS WITH THE NUCLEATOR IN AN OPTICAL DISECTOR

Point-sampled intercepts provide unbiased estimates of the size (volume) of each sampled particle. The necessary uniform position of the sampling point does, however, mean that the estimate in a single particle is quite "noisy", wherefore the distribution of the observations, $\frac{\pi}{3}l_n^3$, in practice is a useless estimate of the distribution of the particle volumes. Estimates made with the nucleator are different. The unique point in the particle, often the nucleolus in the nucleus, may be quite centrally located, and if the cell is not too oddly shaped, the nucleator-estimate of *individual* cell size may be a realistic estimate (and is unbiased in the mean). The distribution of the observations, $\frac{4\pi}{3}l_n^3$, will then be a reasonable approximation of the *real distribution of cell size*. In order to establish this for a

particular cell type one must study the variation of the individual nucleator-estimates of size (volume or surface area) with respect to the *true size* of the *same* cells, a procedure which requires serial sectioning and the use of Cavalieri's estimator for individual cell volume and a spatial, linear test-system on *IUR* sections for surface, see *Sandau* 1987.

When these two different approaches to size estimation are used on the same material it is possible to compare the efficiency of individual estimators, see *Evans et al.* 1989, and *Evans & Gundersen* 1989b where neurons in the human cerebral neocortex have been studied this way. Due to the layered organization of neurons, sampling was carried out on sections perpendicular to the layering in order to reduce the sampling variance, resulting in a vertical section design for estimates of neuron (perikaryon) volume. However, should the vertical section direction deviate from perpendicularity to the layering, how will this effect the variance of the estimator? When neurons were sampled perpendicularly, at 60° , at 30° , and parallel to the layering, respectively, no differences were found in the variation of the nucleator estimate of neuronal volume.

Another problem studied was the number of directions in which to measure the nucleator distance: two directions are always used, but would not 3, 4, or 6 directions be much better? Not surprisingly, there was very little difference in the variation of the nucleator estimate of volume when 3, 4 or 6 systematically selected, *IUR* directions were used. Even more directions are unlikely to be worth the effort as they will all lie in one plane (as long as only a central disector in an ordinary light microscope is used for observations). From a practical point of view, it is therefore recommended that 4 directions be measured for estimation of distributions. Note that on vertical sections *both* the two pairs of opposite directions must be chosen with the direction-finder shown in Fig. 6: the first (systematic) random, the next by adding 48 to the number of the first, otherwise the mean is not unbiased, see *Evans & Gundersen* 1989b for further details. The coefficient of variation associated with a "4-way" nucleator is close to 1.0 when comparing for each neuron the estimate with the (much more elaborate) Cavalieri-estimate obtained from an exhaustive series of optical sections. This is quite acceptable when the coefficient of variation is compared to that of the size distribution of neurons in human temporal neocortex

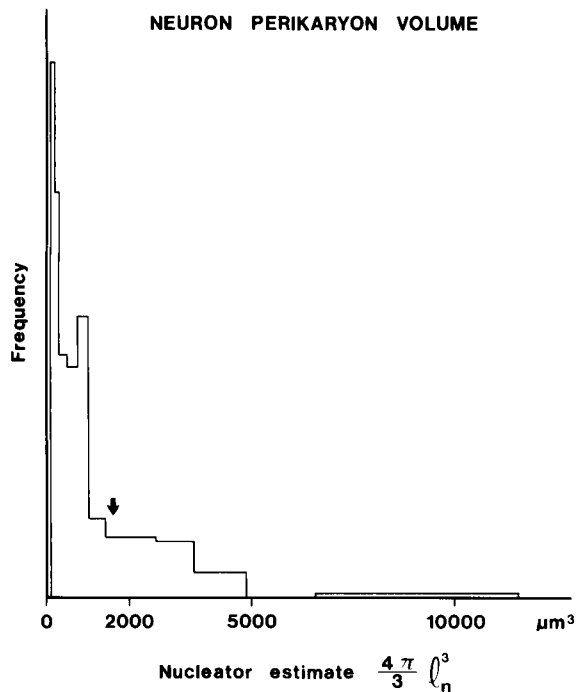


Fig. 10. The neuronal perikaryon volume distribution from the temporal cortex of an 80-year-old man, as estimated by the "4-way" nucleator. The mean neuronal perikaryon size is $1650 \mu\text{m}^3$ (arrow) and a total of 48 cells were measured using a ruler similar to the one shown in Fig. 4, but the widths of the first and the last class were in the ratio 1:50. All layers were sampled uniformly, which is one reason for the relatively large variation in size.

which is about 1.2 to 1.4, see Fig. 10 and Gundersen 1988. This means that the observed variance of the size distribution is a few percent larger than the real variance: the added variance is $\sim \frac{1}{n} \sim 0.01$ when 100 observations are made. It should be pointed out that the *mean* of the observed distribution is the correct mean and that the alternative for volume estimation is serial sectioning, which even with *optical*, serial sections represents a large amount of work.

THE DOUBLE DISECTOR

The following is an example of how one can avoid the non-trivial problem of estimating the thickness of ultrathin sections used in electron microscopy when using the disector to count objects that are small enough to require such thin sections. The specific example used for illustration involves estimating synaptic contacts in the dentate gyrus

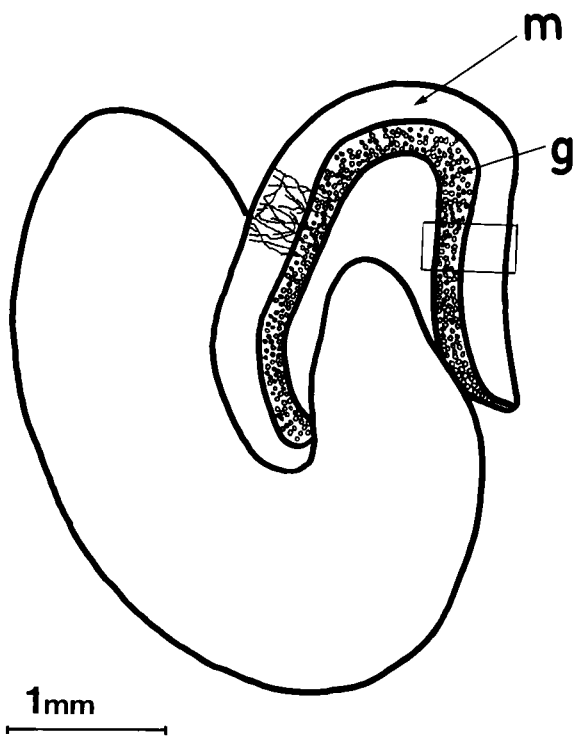


Fig. 11. Diagram of a transverse section of the dentate gyrus in a rat brain. The cell bodies of the mononucleated granule cells are confined to one layer, the granule cell layer (g). The synapses on the dendrites of the granule cells are found in the molecular layer (m). The rectangle on the right shows the outline of a sample for EM.

of the rat brain. The idea is to estimate the numerical density N_V of both synapses and neurons in the same series of ultrathin sections. The ratio of these densities, i.e. the number of synapses per neuron, may then be combined with an estimate of the absolute number of neurons at the light microscopic level to estimate the absolute number of synapses in the region under study. Earlier descriptions of this principle involving the ratio of small to large objects can be found in Gundersen 1986 and Brændgaard & Gundersen 1986.

In the dentate gyrus the neuronal cell bodies are confined to a single layer and their dendritic processes and synapses with afferent fibre systems confined to the adjacent molecular layer, see Fig. 11. The dentate gyrus is cut into 200 to 500 μm thick parallel slabs in the horizontal plane of the brain. Alternate slabs provide material for the Cavalieri-estimate of the reference volume and for the estimate of the synapse to neuron ratio at the

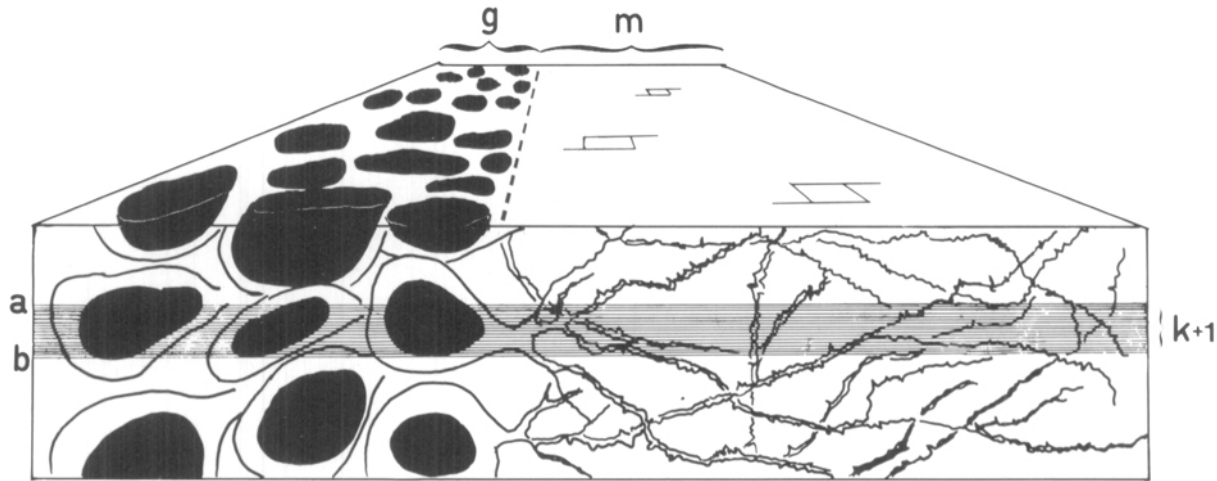


Fig. 12. Diagram summarizing the double disector technique used to estimate the synapse to neuron ratio in a sample as shown in Fig. 11. Serial sections ($k + 1$ in number) are collected from a block containing a sample of the dentate gyrus. The first and last sections (a and b) are used for a disector estimate of the numerical density of neuron nuclei, $N_V(neu/gran)$, in the granule layer. Randomly sampled, adjacent sections within the series are used for the disector estimates of the synapse numerical density in the molecular layer, $N_V(syn/mol)$. Because of the large number of synapses on the dendrites of the granule cells in the molecular layer (m), only a fraction of the area of the molecular layer is sampled in the three small unbiased sampling frames as shown.

electron microscope level. The blocks to be used for *EM* are trimmed from the slabs so that the deep and superficial borders and the arbitrarily defined lateral extents of the layer to be sampled can be observed when ultrathin sections removed from the block are viewed with low power *EM*.

For the estimation of the synapse to neuron ratio in stratified tissue like the dentate gyrus one has to deal with the problem that the neurons and the synapses are in two different reference spaces, the granular and the molecular layers, respectively. It is therefore necessary to estimate the volumes of these two reference spaces separately, which causes no real difficulty. If the two densities are then estimated from uniform samples of the whole of the two reference spaces, granular and molecular layer respectively, the estimate of the number of synapses per neurons is unbiased:¹

$$\frac{N(syn)}{N(neu)} = \frac{\frac{\sum Q-(syn)}{\sum a(syn) \cdot t} \cdot V(mol)}{\frac{\sum Q-(neu)}{\sum a(neu) \cdot k \cdot t} \cdot V(gran)} = \frac{\sum Q-(syn) \cdot \sum a(neu) \cdot k}{\sum Q-(neu) \cdot \sum a(syn)} \cdot \frac{V(mol)}{V(gran)}$$

¹Ratio-estimators with a random variable in the denominator are generally not unbiased, but since the actual bias decreases much faster with increasing number of observations than the *CE* (Jensen & Gundersen 1982) they are considered UFAPP: unbiased for all practical purposes.

where t is the unknown thickness of the ultrathin sections, which cancels nicely in the equation, and k is the known ratio between the number of sections in dissectors for neurons and synapses. In designs such as this example, k equals the number of sections in the disector minus one. $a(syn)$ and $a(neu)$ is the area of the frame used for counting synapses and neurons, respectively. The optimal distance between the sections used in the dissectors is 1 to 2 μm for granule cell nuclei. When a series of relatively thick (gold, ~100 nm) ultrathin sections is used, so that fewer sections are required to obtain the optimal height in the disector, this means that every 10th to 20th section can be used for the neuron dissectors and that one or two random pairs of consecutive sections can be used for the synapse dissectors, see Fig. 12. An estimate of the ratio of synapses to neurons made from a series of sections taken from one block is illustrated by the data in Table 3. A series of 15 sections was used. Corresponding fields of vision on adjacent sections of three systematic, randomly selected areas of the molecular layer were used for the synapse disector samples. The analyses were performed in both directions by interchanging the roles (sampling and look-up sections) of the top and bottom sections in the dissectors, see Fig. 13. This doubles the sample size with very little extra

TABLE 3. Hippocampal granule cells and synapses sampled in a double disector

Disector sample	Q^- (top)	Q^- (bottom)	Σ
Granule cells	22	21	43
Synapses, I	9	18	27
Synapses, II	8	17	25
Synapses, III	12	16	28
Synapses, Total			80

$$a(neu) = 0.013 \text{ mm}^2$$

$$a(syn) = 5.42 \cdot 10^{-5} \text{ mm}^2$$

$$\frac{V(mol)}{V(gran)} = \frac{11.47 \text{ mm}^3}{3.08 \text{ mm}^3} = 3.72$$

$$\frac{N(syn)}{N(neu)} = \frac{\Sigma Q^-(syn) \cdot \Sigma a(neu) \cdot k}{\Sigma Q^-(neu) \cdot \Sigma a(syn)} \cdot \frac{V(mol)}{V(gran)}$$

$$= \frac{80 \cdot 2 \cdot 0.013 \cdot 14}{43 \cdot 6 \cdot 0.0000542} \cdot 3.72 = 7700$$

Neurons and synapses counted in the granular layer of rat hippocampus using double dissectors as shown in Fig. 12. Synapses are counted in three frames, each of area $a(syn) = 5.42 \cdot 10^{-5} \text{ mm}^2$. The ratio of the two reference volumes are from *Coleman et al.* 1987.

effort and the same particle cannot thereby be counted twice! In practice, one should probably have at least two to four dissectors uniformly sampled in the reference space, more if inhomogeneity is detectable in the sample.

In situations where the study concerns *localized* changes due to local stimuli such a simple and strong design is unfortunately not possible. This raises the tricky problem of the correspondence: are the synapses in the molecular layer just above a certain region of the granular layer the synapses from the neurons in that particular region of the granular layer? Equally critical: is the delineation by two parallel lines perpendicular to the pial surface as in Fig. 11 a proper definition of the correspondence? There are no general answers to these questions, great caution must be exercised in order to avoid the "reference trap" of which some classical examples are given in *Brændgaard & Gundersen* 1986. See also the recent work by *Cadete-Leite et al.* 1988 who drew conclusions from estimates of the *density* of neurons in the granule layer in the hippocampus. Their conclusion (drawn in the title of the paper) was warranted only because they also measured the *thickness* of the granule cell layer, i.e. they had a reasonable measure of the marked change in the volume of the reference space.

Even after uniform sampling, the synapse to neuron ratio may not always be an adequate descriptor. In situations in which one cannot safely assume that the number of neurons is constant, conclusions drawn from differences in the synapse to neuron ratio may not be valid. When synaptic changes may occur and there is not adequate time for neuronal changes, such as the acute effects of drugs or physiological stimuli, it may be valid to make assumptions about the absence of changes in neuronal number and the synapse to neuron ratio can be a valuable parameter. Similarly, in situations in which one wishes to investigate distributional differences, such as gradients in the innervation or localized effects of lesions or transplants, synapse to neuron ratios may clearly be of some value despite difficulties in general in interpreting the data rigorously.

ANOTHER DOUBLE DISECTOR IN A PHYSICAL-OPTICAL COMBINATION

What is described here is a principle which allows the unbiased estimation of all cells (endothelial, epithelial, mesangial and – if present – inflammatory cells) in an average glomerulus without regard to shrinkage and section thickness. The basic

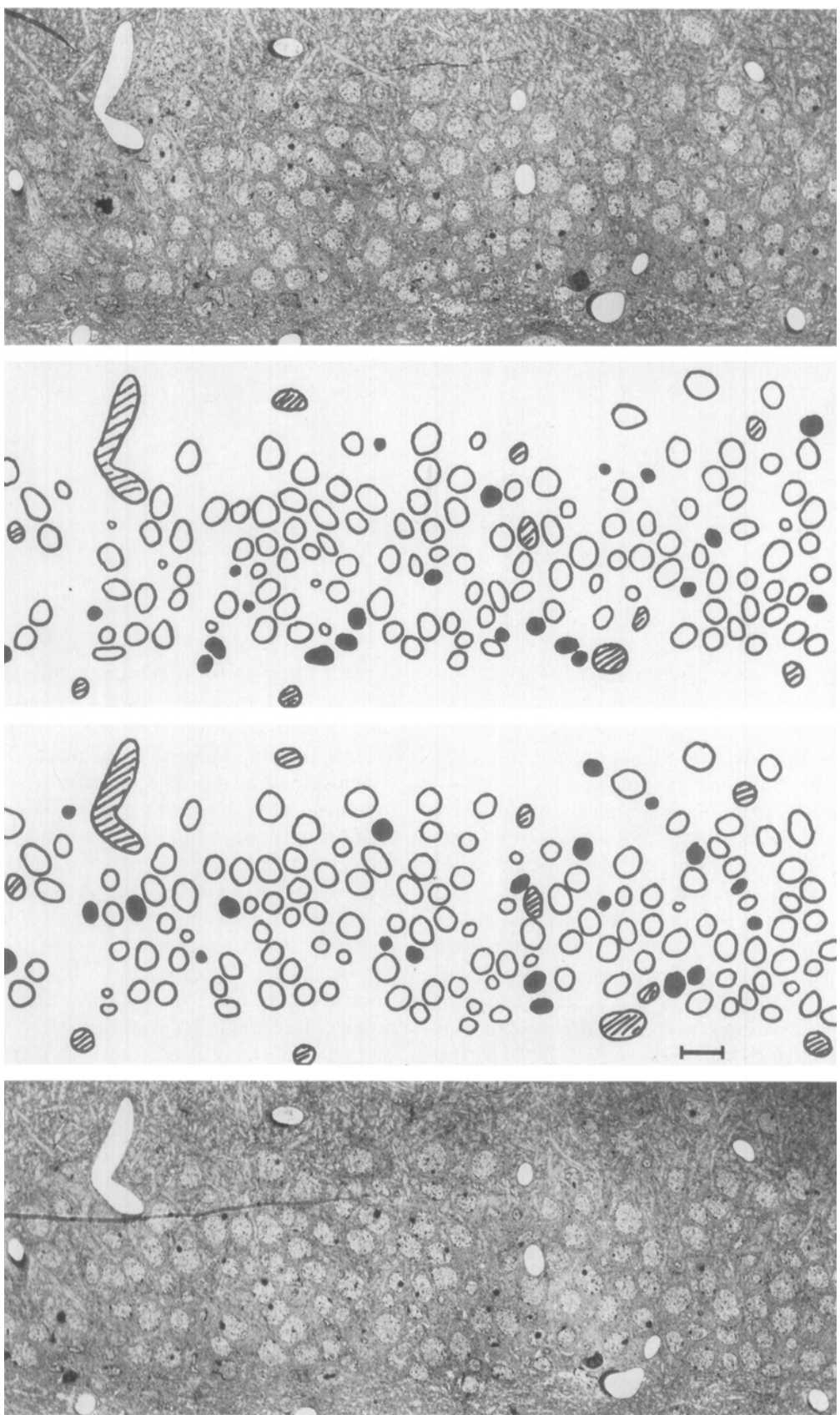


Fig. 13. Low power electron micrographs of the granule cell layer of the 1st and 15th sections in the series with outlines of the nuclei of the granule cells in the interposed drawings. The nuclei which appear in one section and not in the other are in black: $Q^- = 22$ in the upper section and 21 in the lower, see Table 3. The blood vessels are hatched. Bar is 10 μm .

principle is to estimate separately the numerical density of cells in the glomeruli $N_N(\text{cells/glom})$ and the mean glomerular volume $\bar{v}(\text{glom})$. By definition

$$N_N(\text{cells/glom}) = N_V(\text{cells/glom}) \cdot \bar{v}(\text{glom})$$

The containing or reference space for $N_V(\text{cells/glom})$ must be measured in the same units as $\bar{v}(\text{glom})$, both formally and actually. The simplest and best way to do this is to make both estimates in the same sections. The units may then be

arbitrary and unknown, and shrinkage and other dimensional deformation of the glomeruli or of the cells become irrelevant. The estimation of $N_N(\text{cells/glom})$ can be performed in kidney biopsies as well as in material from whole kidneys. Slightly different stereological methods, but based on the same principle, are used for plastic and paraffin embedded material, see *Marcussen et al.* 1989. For illustration, estimation of $N_N(\text{cells/glom})$ in autopsy kidney tissue embedded in paraffin is briefly described, the method also applies to biopsies with only trivial modifications.

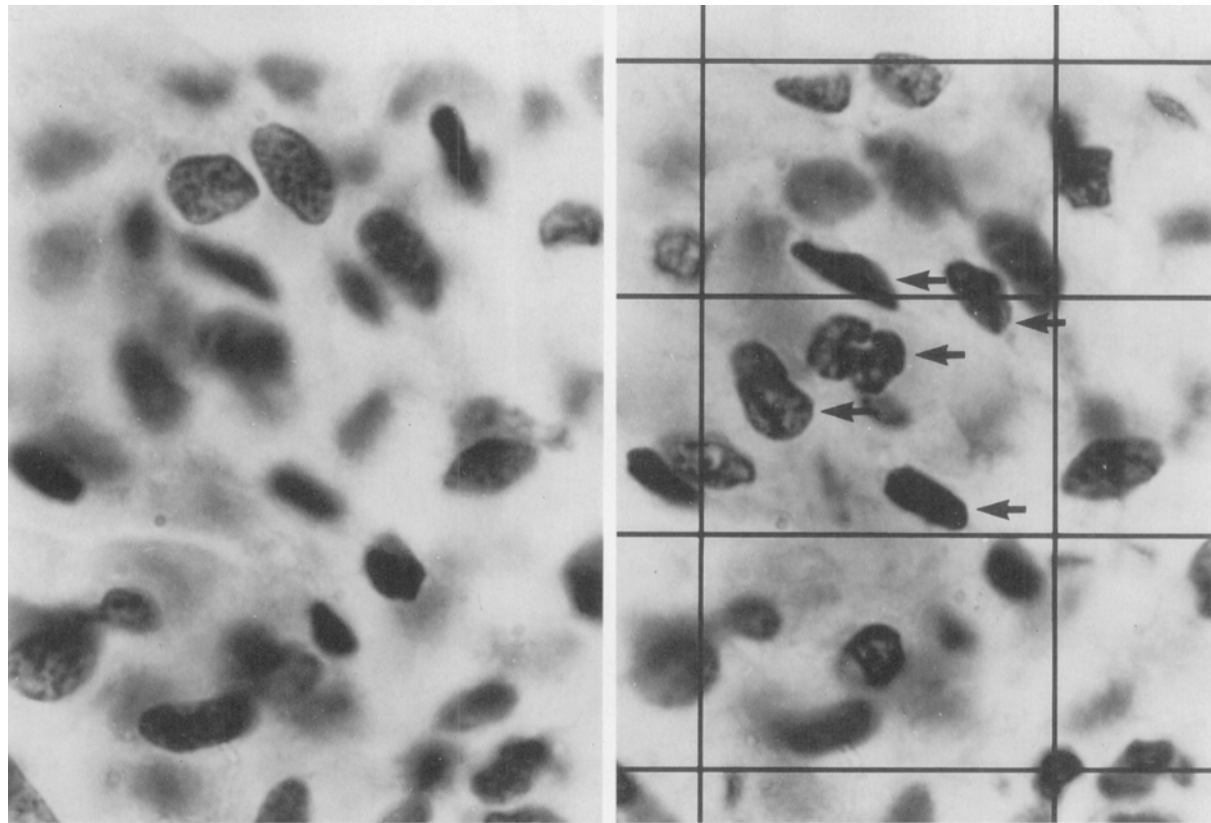


Fig. 14. Two optical section planes through a glomerulus with a distance of approximately 3 μm . The distance is illustrated by the thickness of the separation line between the two pictures. To the left is the top look-up plane and the nuclei clearly seen here are not counted. Moving 3 μm towards the bottom five new nuclei come into focus in the central rectangle and are counted (right). A part of the randomly thrown tessellation of counting frames each of an area 18 $\mu\text{m} \cdot 28 \mu\text{m} = 504 \mu\text{m}^2$ is seen. Two unbiased counting frames in each glomerulus were used for counting through the whole section thickness. Hematoxylin-Giemsa stained.

Four slices of a few mm thickness were systematically sampled from a formalin fixed autopsy kidney. The slices were embedded in paraffin and two Hematoxylin-Giemsa stained $\sim 25 \mu\text{m}$ thick sections were made from each. A glomerulus was defined as the minimal convex figure enclosing the glomerular tuft. $N_V(\text{cells/glom})$ was estimated in an optical disector. The glomeruli were randomly sampled by moving perpendicularly from the capsule through the cortex to the medulla and back again using a stage drive. The fields of vision were projected onto the table using a projection microscope, see Fig. 3, and every fifth glomerular profile was chosen for subsampling at a high magnification using a $100X$ oil immersion objective with 1.40 NA. On the table a tesselation of counting frames, each of area a_1 , was placed randomly. Using a table of random numbers, two test frames were counted in each selected glomerulus. The look-up plane was defined as the two-dimensional section plane where the nuclei were first seen clearly when focusing from top to bottom in the section. All nuclei which were not intersected by the look-up plane were counted, see Fig. 14. A total of approximately 150 to 200 cells were counted in roughly 15 glomeruli. The average numerical density of cells in glomeruli is now $N_V(\text{cells/glom}) = \Sigma Q^-(\text{cells})/(t \cdot \Sigma a_1)$ where t is the unknown thickness of the section. Using the pair of $\sim 25 \mu\text{m}$ thick sections as a physical disector one estimates

$$\bar{v}(\text{glom}) = \frac{V_V(\text{glom/cortex})}{N_V(\text{glom/cortex})} = \frac{P_p(\text{glom/cortex})}{N_V(\text{glom/cortex})}$$

where $V_V(\text{glom/cortex})$ is the volume fraction of glomeruli in the cortex estimated by point counting using a $10X$ objective on one section of the disector-pair and $N_V(\text{glom/cortex})$ is the numerical density of glomeruli in the cortex. In a pilot study it was found that, at this magnification and in such thick sections overprojection and so-called "lost

caps" were a minor problem when estimating glomerular volume (see Møller 1986 for another estimator of glomerular number using just fixed tissue cut in a vibratome). A stage drive was used to move the unbiased counting frame of area a_2 through the cortex from the capsule to the medulla. $10X$ objectives and two fields of vision from two identical projection microscopes were used. As before $N_V(\text{glom/cortex}) = \Sigma Q^-(\text{glom})/(t \cdot \Sigma a_2)$ where t is the same unknown thickness of the section which therefore cancels when combining the above equations

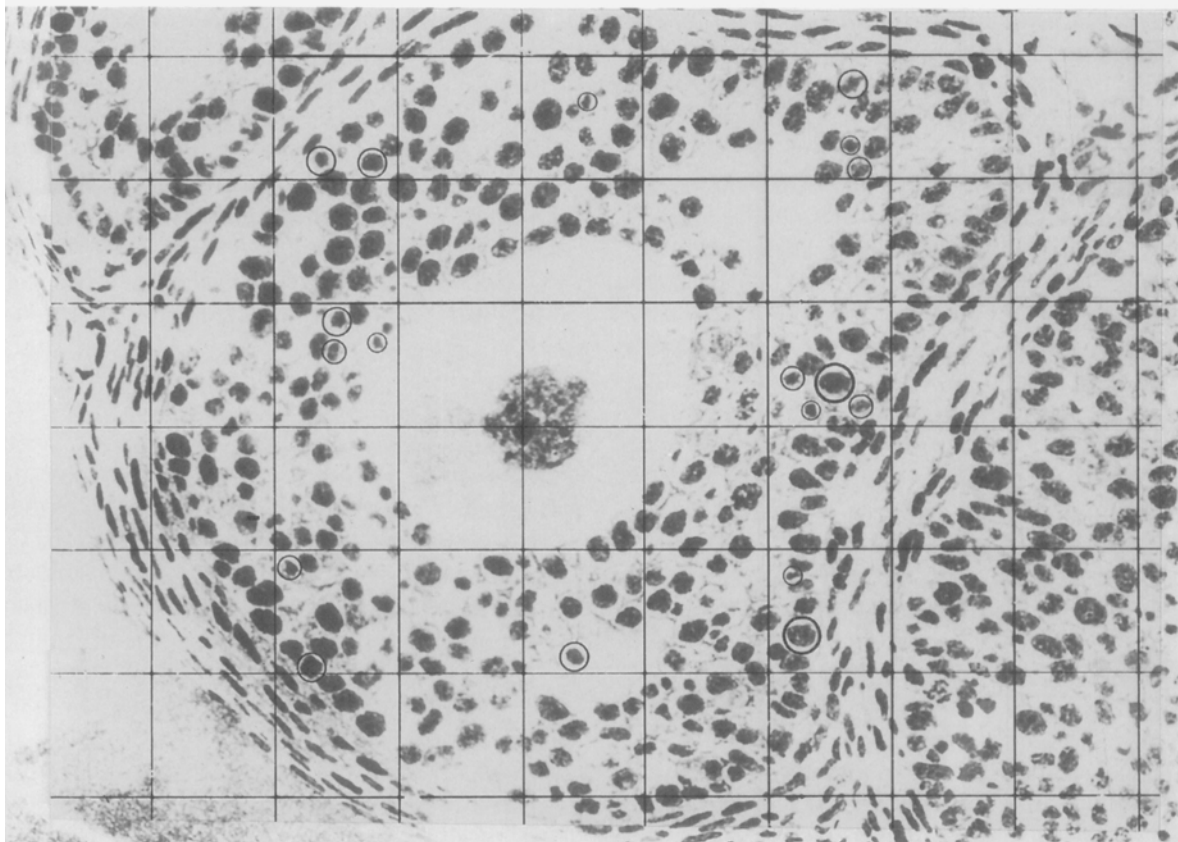
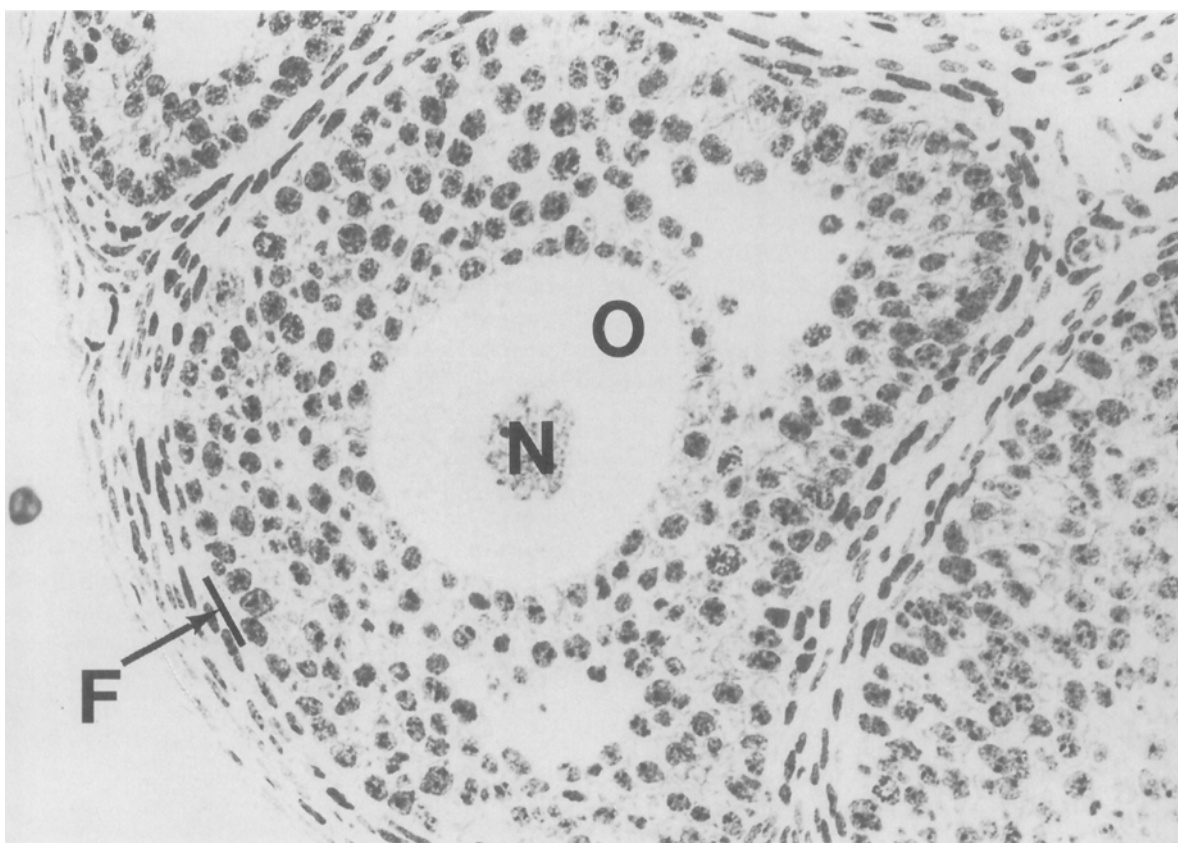
$$N_V(\text{cells/glom}) = \frac{\Sigma Q^-(\text{cells}) \cdot \Sigma a_2}{\Sigma Q^-(\text{glom}) \cdot \Sigma a_1} \cdot P_p(\text{glom/cortex})$$

The last term is, of course, just the ratio between the two reference volumes as in the double disector for estimating the number of synapses per neuron. A normal human glomerulus contains ~ 2500 cells. If it is also necessary to know the number of *each* type of cells in the glomeruli, differential counting has to be performed. This is best done in thin sections in a physical disector using e.g. silver staining as shown below for the follicle in Fig. 15.

The main disadvantage of the method is that one has to make certain that "lost caps" are not a problem because the entire thickness of the section is used as the sampling space for the disector-counting of cells in glomeruli. If nuclei have dropped out of the bottom plane of the section, one underestimates the numerical density, a phenomenon which does *not* affect counting in a disector which employs *two* section planes (Sterio 1984) or in an optical disector with measured height (Gundersen 1986) where one, for precisely that reason, avoids the bottom of the section. The magnitude of the bias is not known, but considering that $\sim 25 \mu\text{m}$ sections were used it is unlikely to be of much practical importance. In plastic sections it is probably not present at all.

Fig. 15. Two adjacent glycolmethacrylate sections of $1 \mu\text{m}$ thickness through a mouse ovary. The orientation of the section pair is made isotropic through the use of Mattfeldt's Orientator (See APMIS-1). The pair is selected from a number of parallel sections because the lower section is the first to hit the nucleolus of the oocyte. A quadratic test system is placed *arbitrarily* on the section with a corner on the nucleolus. In a systematic random quarter of all frames all granulosa cell nuclear profiles are sampled obeying the unbiased 2-dimensional counting rule, see Fig. 2. The 20 profiles through nuclei which are *not* seen in the upper section are encircled on the lower section. The staining used is a silver stain developed by Danscher 1983. The distance between the test lines is $34 \mu\text{m}$ at the tissue level, the width of the white strip separating the micrographs is $1 \mu\text{m}$. Notice that the nuclei are not rarely separated by less than $1 \mu\text{m}$, a feature which makes it difficult to identify them unambiguously and therefore sample them unbiasedly using a disector of two physical sections. Using *optical* disectors this is, however, not a problem at all. F, O, and N indicate the follicles' limit towards the theca, the oocyte, and the oocyte nucleus, respectively.

THE NEW STEREOLOGICAL TOOLS



THE NUMBER OF BALLS IN A NUCLEATED BAG

This final example is the only one in this review where some critical information depends on knowledge of the section thickness. As illustrated by most of the above examples, a lot of effort and ingenuity (e.g. the Selector!) have been put into the development of methods over the last four years which eliminate the need to know the disector height, h . Another example of this is the procedure described in *Pakkenberg & Gundersen* 1988, where a disector-Cavalieri combination eliminates section thickness. As mentioned above, the use of *optical* dissectors does, however, to a very large extent solve the problem in general.

Fig. 15 shows an ovarian follicle from a mouse. To reproduction-biologists such a section represents a large amount of potential information: what are the volumes of the oocyte, its nucleus, the antrum, i.e. the excentric cavity (cavities?) and of the whole follicle? These answers can be obtained in a straightforward manner with the nucleator, since the follicle has an easily recognizable and unique unit in the middle, the nucleolus of the oocyte. Unbiased estimates of these volumes in this particular follicle are: $v(\text{follicle}) = 5.16 \cdot 10^6 \mu\text{m}^3$, $v(\text{oocyte}) = 0.33 \cdot 10^6 \mu\text{m}^3$, $v(\text{oocyte nucleus}) = 9930 \mu\text{m}^3$, $v(\text{antrum}) = 0.36 \cdot 10^6 \mu\text{m}^3$. In order to obtain these estimates, the section which happens to hit the nucleolus was selected from a stack with isotropic orientation. This also means that most other stereological estimators *cannot* be used because they require the section to be uniformly random in position – and the particular section which hits the oocyte nucleolus is definitely not in a random position with respect to the well-ordered little universe of a follicle. Using the two consecutive sections shown in Fig. 15 as a disector of height $h = 1 \mu\text{m}$ we may, for example, think about estimating the number of granulosa cell nuclei in the sampled space of volume = $h \cdot (\text{follicle cross sectional area})$. Sampling in a systematic, random quarter of the frames, there are 20 nuclei hit by the section but not by the previous one, i.e.

$$N_v(\text{gran.cells/follicle central volume}) \sim \frac{20}{7 \cdot (15000)^2} = 2.46 \cdot 10^{-3} \mu\text{m}^{-3}$$

where 7 is the number of upper frame corners hitting the follicle, the frame area is 15 by 15 mm, and the magnification is 440X. Unfortunately, this

figure of ~ 2.5 granule cell per $1000 \mu\text{m}^3$ is *not* the numerical density N_V (*gran.cells/follicle*) of granulosa cells in the follicle – because the disector is not uniformly positioned in the follicle.

Then, what *is* the total number of granulosa cells in the follicle and how can we estimate that number by just observing one central and thereby arbitrarily positioned disector? The number of granulosa cells is clearly related to the total number counted in the disector, i.e. $4 \cdot Q^- = 4 \cdot 20$, a number which is in turn directly proportional to the height $h = 1 \mu\text{m}$ of the disector: if h were e.g. 2 μm , for example, we would expect Q^- to be 160, and so on. The problem is, that since the disector has an *isotropic* orientation and passes through the nucleolus, a granulosa cell close to the nucleolus has a greater chance of being sampled (and counted) in the disector than another cell which is more distant from the nucleolus. The probability that the i 'th granulosa cell is counted in the disector is therefore proportional to h and inversely proportional to the distance d_i from the nucleolus (the centre for the disector-rotation in space) to the granulosa cell nucleus:

$$\text{Prob(counting granulosa cell)} = \frac{1}{d_i} \cdot \frac{h}{2}$$

This is a unique feature: *after* having counted the i 'th granulosa cell we can estimate its *a priori* probability of being captured by the probe (the disector) from measurements made in the probe itself! No other case of this is known in Stereology. It is now but a simple matter of inverting the above probability and summing over all n cells counted to provide an *unbiased estimator of the total number of granulosa cell nuclei in the follicle under study*:

$$N(\text{gran. cells/follicle}) = \frac{2 \cdot \sum_{i=1}^n d_i}{h} = \frac{2 \cdot 4 \cdot 0.757 m \cdot 10^6}{1 \mu\text{m} \cdot 440} = 13.700$$

The factor of 4 is related to the sampling scheme in which only a quarter of all cells in the disector pair were sampled in the example in Fig. 15. The constant 2 is specific for isotropically oriented sections. If vertical sections are used, the constant is π , and d_i is the shortest distance from the i 'th granulosa cell to the vertical axis (which passes through the nucleolus). For proofs of the above relations and a more detailed description of the method, see *Bagger et al.* 1988.

Like the other estimators based on the nucleator principle the estimator of total number of particles

per universe is an unbiased estimator *independent of the shape of the universe, the position of the unique point, and of the shape, size and position of the particles to be counted*. The complete cross section of the universe must of course be observable in the section where the unique point is seen. On the other hand, the statistical variation of the estimate, CE , clearly depends on all these factors and is also likely to vary inversely with the absolute number of granulosa cells sampled in the disector. Only the last factor is known and leads to an estimated $CE = \frac{1}{\sqrt{20}} \sim 0.22$ which is then a lower limit for the real CE in the example. If we want a more precise estimate we may sample *all* cells in the central disector instead of a quarter of them and, moreover, use a greater height in the disector. There is, however, likely to be a narrow limit as to how efficient these improvements really are: they do not decrease the contribution to the real CE from all the other factors mentioned above. Also, taking into consideration the biological variation between different follicles at the same stage of development and the fact that scientific statements therefore must be based on a *sample* of such follicles, it is obvious that an optimal sampling strategy involves a certain number of follicles and only a relatively small number of measurements in each. As opposed to more measurements per follicle, more follicles (n , say) in the sample reduces the contribution of *all* sources to the CE of the estimated mean by a factor $\frac{1}{\sqrt{n}}$. The optimal division of the sampling effort in follicles at varying stages is currently under study, see *Bagger et al.* 1988.

Finally, according to Evans' idea (*Evans & Gundersen* 1989a) the section pair in Fig. 15 also contain all the necessary information to obtain an estimate of the *3-dimensional spatial distribution* of all elements of the follicle with respect to the oocyte nucleolus. There are, for example, a rather large number of granulosa cells in various stages of mitosis. Are these cells uniformly distributed among the granulosa cells in the 3-dimensional space of the follicle or is it, for example, mainly the most peripheral cells which are dividing? The unique feature of the nucleator which we can exploit here is that the 3-dimensional *distance* from the oocyte nucleolus to everything in the follicle is observable in the section. It is therefore not only possible to estimate correctly the fraction of cells in mitosis but also *the variation of the mitotic index* = $\frac{\# \text{ mitoses}}{\# \text{ cells}}$ as a function of the distance,

SPATIAL DISTRIBUTION OF GLIA AROUND NEURONS

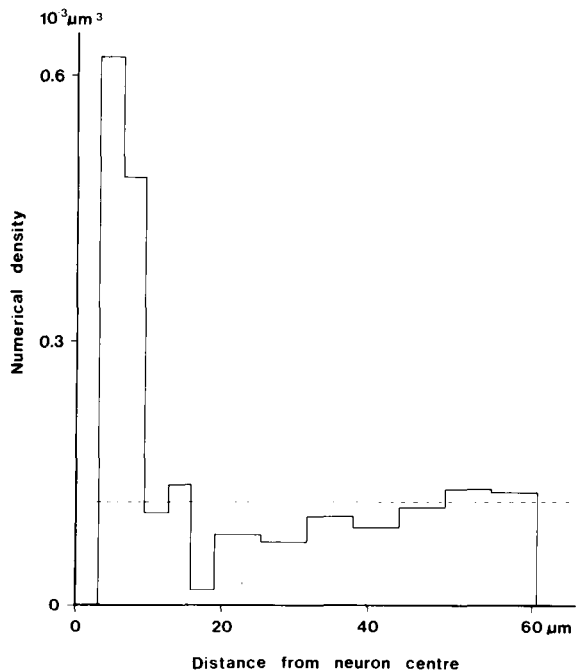


Fig. 16. The variation in the local numerical density of glia cells as a function of the distance from a neuron nucleolus. Thirty neurons were sampled from human temporal cortex in isotropic sections and a total of 145 glia cells were counted in a design as shown in Fig. 15 but in optical disectors using the microscope in Fig. 3 (*Evans & Gundersen* 1989a). The graph clearly illustrates that there is a lower limit to how close glia cells can be to a neuron nucleolus – the radius of the neuron! – and that just outside the neuron there is a concentration of glia cells which is about five times higher than the overall numerical density of ~ 1.1 glia cell per $10.000 \mu\text{m}^3$. Outside this crowd of glia cells around a neuron there may even be a zone at about a distance of $20 \mu\text{m}$ with a particularly low density of glia cells.

i.e. its spatial distribution. Fig. 16 illustrates the analogous function of the numerical density of glia cells in relation to neurons in human neocortex; this can be compared to Fig. 4.

Pathologists like oceanographers and mining engineers never forget that their objects are 3-dimensional – words like intercellular space, invasion, and hypervasculatization lose their meaning if applied to the *section* rather than to the cells and the tissue. The purpose of this review has been to show that when diagnosis or research needs to sharpen its aim by quantitating the maybe subtle

3-dimensional changes which might be decisive – then there are handy and well understood instruments already developed for precisely that purpose.

The dedicated technical assistance of *S. Bergman, M. D. Christiansen, D. Da Silva, E. Kabell-Kjær, A. Larsen, M. Lundorff, A. Nielsen, L. Nielsen, P. E. Nielsen & P. Schirmer* is thankfully acknowledged.

REFERENCES

- Bagger, P. V., Bang, L., Christiansen, M. D., Gundersen, H. J. G., Kabell-Kjær, E. & Mortensen, L.*: Total number of particles in a bounded region estimated directly using the nucleator: Granulosa cell number in ovarian follicles. To be published, 1989.
- Bendtsen, T. F. & Nyengaard, J. R.*: Unbiased estimation of particle number using sections – a historical perspective with special reference to the stereology of glomeruli. In press *J. Microsc.*, 1988.
- Brüniger, A. & Cruz-Orive, L. M.*: Nuclear morphometry of nodular malignant melanomas and benign neovascular nevi. *Arch. Dermatol. Res.* 279: 412-414, 1987.
- Brændgaard, H. & Gundersen, H. J. G.*: The impact of recent stereological advances on quantitative studies of the nervous system. *J. Neurosci. Meth.* 18: 39-78, 1986.
- Brændgaard, H., Evans, S. M., Howard, C. V. & Gundersen, H. J. G.*: An unbiased method for estimating the total number of neurons in the human neocortex using the disector. To be published, 1989.
- Cadete-Leite, A., Tavares, M. A. & Paula-Barbosa, M. M.*: Alcohol withdrawal does not impede hippocampal granule cell progressive loss in chronic alcohol-fed rats. *Neurosci. Lett.* 86: 45-50, 1988.
- Calverley, R. K. S. & Jones, D. G.*: Determination of the numerical density of perforated synapses in rat neocortex. *Cell. Tiss. Res.* 248: 399-407, 1987.
- Coleman, P. D., Flood, D. G. & West, M. J.*: Volumes of the components of the hippocampus in the aging F344 rat. *J. Comp. Neurol.* 266: 300-306, 1987.
- Cruz-Orive, L.-M.*: Particle number can be estimated using a disector of unknown thickness: The selector. *J. Microsc.* 145: 121-142, 1987.
- Danscher, G.*: A silvermethod for counterstaining plastic embedded tissue. *Stain Technology* 58: 356-372, 1983.
- Diem, K. & Lentner, C.*: *Documenta Geigy. Scientific Tables*. J. R. Geigy, Basel, 1970.
- Evans, S. M. & Gundersen, H. J. G.*: Unbiased and general stereological estimators of 3-dimensional distributions of distances and densities using the nucleator. To be published, 1989a.
- Evans, S. M., Sandau, K., Jensen, E. B. & Gundersen, H. J. G.*: A comparison of two unbiased estimators of individual particle surface area. To be published, 1989.
- Gundersen, H. J. G.*: Stereology of arbitrary particles. A review of unbiased number and size estimators and the presentation of some new ones, in memory of William R. Thompson. *J. Microsc.* 143: 3-45, 1986.
- Gundersen, H. J. G.*: The nucleator. In press. *J. Microsc.* 150: 1988.
- Gundersen, H. J. G. & Jensen, E. B.*: Particle sizes and their distributions estimated from line- and point-sampled intercepts. Including graphical unfolding. *J. Microsc.* 131: 291-310, 1983.
- Gundersen, H. J. G. & Jensen, E. B.*: Stereological estimation of the volume-weighted mean volume of arbitrary particles observed on random section. *J. Microsc.* 138: 127-142, 1985.
- Gundersen, H. J. G. & Jensen, E. B.*: The efficiency of systematic sampling in stereology and its prediction. *J. Microsc.* 147: 229-263, 1987a.
- Gundersen, H. J. G. & Jensen, E. B.*: Estimation of moments of size distributions of arbitrary particles. *Acta Stereol.* 6: 197-199, 1987b.
- Gundersen, H. J. G., Bendtsen, T. F., Korbo, L., Marcussen, N., Møller, A., Nielsen, K., Nyengaard, J. R., Pakkenberg, B., Sørensen, F. B., Vesterby, A. & West, M. J.*: Some new, simple and efficient stereological methods and their use in pathological research and diagnosis. *APMIS* 96: 379-394, 1988.
- Helander, K., Hofer, P.-Å. & Hollmberg, G.*: Karymetric investigations on urinary bladder carcinoma, correlated to histopathological grading. *Virchows Archiv A* 403: 117-125, 1984.
- Howard, V.*: Rapid nuclear volume estimation in malignant melanoma using point sampled intercepts in vertical sections: A review of the unbiased quantitative analysis of particles of arbitrary shape. In: *Mary, J. Y. & Rigaut, J. P.* (Eds.): *Quantitative Image Analysis in Cancer Cytology and Histology*. Elsevier Science Publisher, New York 1986, pp. 245-254.
- Howard, V., Reid, S., Baddeley, A. & Boyde, A.*: Unbiased estimation of particle density in the tandem scanning reflected light microscope. *J. Microsc.* 138: 203-212, 1985.
- Jensen, E. B. & Gundersen, H. J. G.*: Stereological ratio estimation based on counts from integral test systems. *J. Microsc.* 125: 51-66, 1982.
- Jensen, E. B., Kéti, K. & Gundersen, H. J. G.*: On stereological estimation of moment measures. In: Research Report No. 175, 1988, pp. 1-20. Department of Theoretical Statistics, University of Aarhus, Aarhus.
- Jolly, G. M.*: Sampling of large objects. In: *Cormack, R. M., Patil, G. P. & Robson, D. S.* (Eds.): *Sampling Biological Populations*. Int. Co-operat. Publish. House, Maryland 1979, pp. 193-201.
- Marcussen, N., Christensen, S., Gundersen, H. J. G. & Ottosen, P. D.*: Unbiased stereological estimation of the number of particles inside other particles, with a comparison of estimators of size and size distributions. In preparation, 1989.

- Michel, R. P. & Cruz-Orive, L.-M.*: Application of the Cavalieri principle and vertical sections method to lung: Estimation of volume and pleural surface area. *J. Microsc.* 150: 117-136, 1988.
- Mulvany, M. J., Baandrup, U. & Gundersen, H. J. G.*: Evidence for hyperplasia in mesenteric resistance vessels of spontaneously hypertensive rats using a three-dimensional disector. *Circ. Res.* 57: 794-800, 1985.
- Møller, A. & Gundersen, H. J. G.*: Estimation of cell size using the nucleator - with justification of a number of efficient modifications applied in neuroscience. In preparation, 1989.
- Møller, J. C.*: Dimensional changes of proximal tubules and cortical capillaries in chronic obstructive renal disease. *Virchows Arch. A.* 410: 153-158, 1986.
- Nielsen, K., Colstrup, H., Nilsson, T. & Gundersen, H. J. G.*: Stereological estimates of nuclear volume correlated with histopathological grading and prognosis of bladder tumour. *Virchows. Arch. (Cell. Pathol.)* 52: 41-54, 1986.
- Nielsen, K., Berild, G. H., Bruun, E., Jørgensen, P. E. & Weis, N.*: Stereological estimation of mean nuclear volume in prostatic cancer, the reproducibility and the possible value of estimations on repeated biopsies in the course of disease. In press *J. Microsc.*, 1988a.
- Nielsen, K., Ørntoft, T. & Wolf, H.*: Stereological estimates of nuclear volume in non-invasive bladder tumors (Ta) correlated with the recurrence pattern. In press *J. Urol.*, 1988b.
- Nyengaard, J. R. & Bendtsen, T. F.*: Glomerular number in a wide range of animals estimated by a simple and unbiased stereological method. To be published 1989a.
- Nyengaard, J. R. & Bendtsen, T. F.*: Number and size of glomeruli, kidney weight and body surface in normal human beings. To be published 1989b.
- Ooms, E. C. M., Blok, A. P. R. & Veldhuizen, R. W.*: The reproducibility of a quantitative grading system of bladder tumours. *Histopathology* 9: 501-509, 1985.
- Pakkenberg, B. & Gundersen, H. J. G.*: Total number of neurons and glia cells in human brain nuclei estimated by the disector and the fractinator. *J. Microsc.* 150: 1-20, 1988.
- Petran, M., Hadravsky, M., Egger, M. D. & Galambos, R.*: Tandem-Scanning Reflected-Light Microscope. *J. Opt. Soc. Am.* 58: 661-664, 1968.
- Sandau, K.*: How to estimate the area of a surface using a spatial grid. *Acta Stereologica 6/III*: 31-36, 1987.
- Sterio, D. C.*: The unbiased estimation of number and sizes of arbitrary particles using the disector. *J. Microsc.* 134: 127-136, 1984.
- Sørensen, F. B.*: Stereological estimation of nuclear volume in benign melanocytic lesions and cutaneous malignant melanomas. Submitted 1989a.
- Sørensen, F. B.*: Objective histopathological grading of cutaneous malignant melanomas by stereological estimation of nuclear volume: Prediction of survival and disease-free period. Submitted 1989b.
- Sørensen, F. B.*: Stereological estimation of volume- and number-weighted mean nuclear volume from vertical sections of benign and malignant nuclear populations with analysis of size-variability. In preparation 1989c.
- Vesterby, A.*: Unbiased estimation of the number of osteoclasts in iliac crest biopsies. In preparation 1989.